$\mathcal{S}$

ENGINEERING CHANGE NOTICE	1. ECN 648613
Page 1 of 2	Proj. ECN

2. ECN Category (mark one)	3. Originator's Name, Organization, MSIN, and Telephone No.	4. USQ Required?	5. Date
Supplemental [] Direct Revision [X] Change ECN [] Temporary [] Standby [] Supersedure [] Cancel/Void []	D. E. Ball, Process Engineering, R3-86, 373-0615	[] Yes [X] No	October 13, 1998
	6. Project Title/No./Work Order No.	7. Bldg./Sys./Fac. No.	8. Approval Designator
	Spent Nuclear Fuel	N/A	S, Q
	9. Document Numbers Changed by this ECN (includes sheet no. and rev.)	10. Related ECN No(s).	11. Related PO No.
	HNF-1523, Rev 0	N/A	N/A

12a. Modification Work	12b. Work Package No.	12c. Modification Work Complete	12d. Restored to Original Condition (Temp. or Standby ECN only)
[] Yes (fill out Blk. 12b) [X] No (NA Blks. 12b, 12c, 12d)	N/A	N/A Design Authority/Cog. Engineer Signature & Date	N/A Design Authority/Cog. Engineer Signature & Date

13a. Description of Change   13b. Design Baseline Document? [] Yes [X] No

Complete document revision. The analysis, FAI/97-90 Rev 4, attached to HNF-1523, Rev 0 has been replaced by FAI/98-97 Rev 3. This new analysis provides updated MCO water inventory estimates based on revised MCO particulate inventory estimates and eliminates follow-on calculations of MCO pressure and gas composition. The calculations of MCO pressure and gas composition can now be found in HNF-SD-SNF-TI-040.

14a. Justification (mark one)

Criteria Change	[X]	Design Improvement	[]	Environmental	[]	Facility Deactivation	[]
As-Found	[]	Facilitate Const	[]	Const. Error/Omission	[]	Design Error/Omission	[]

14b. Justification Details

Updated values for particulate inventory estimates were provided in HNF-1527, Rev 2 and these are reflected in this revision. In addition, the redundancy of providing MCO pressure responses in two documents was eliminated.

15. Distribution (include name, MSIN, and no. of copies)

See Page 2 of this ECN for Approval signatures.
See attached Distribution sheet for distribution.

RELEASE STAMP

DATE
STA: H
OCT 23 1998
HANFORD RELEASE
ID: 58

A-7900-013-2 (05/96) GEF095

A-7900-013-1

ENGINEERING CHANGE NOTICE

	1. ECN (use no. from pg. 1)
	648613

16. Design Verification Required	17. Cost Impact				18. Schedule Impact (days)	
	ENGINEERING		**CONSTRUCTION**			
[ ] Yes	Additional	[ ] $	Additional	[ ] $	Improvement	[ ]
[X] No	Savings	[ ] $	Savings	[ ] $	Delay	[ ]

19. Change Impact Review: Indicate the related documents (other than the engineering documents identified on Side 1) that will be affected by the change described in Block 13. Enter the affected document number in Block 20.

SDD/DD	[ ]	Seismic/Stress Analysis	[ ]	Tank Calibration Manual	[ ]
Functional Design Criteria	[ ]	Stress/Design Report	[ ]	Health Physics Procedure	[ ]
Operating Specification	[ ]	Interface Control Drawing	[ ]	Spares Multiple Unit Listing	[ ]
Criticality Specification	[ ]	Calibration Procedure	[ ]	Test Procedures/Specification	[ ]
Conceptual Design Report	[ ]	Installation Procedure	[ ]	Component Index	[ ]
Equipment Spec.	[ ]	Maintenance Procedure	[ ]	ASME Coded Item	[ ]
Const. Spec.	[ ]	Engineering Procedure	[ ]	Human Factor Consideration	[ ]
Procurement Spec.	[ ]	Operating Instruction	[ ]	Computer Software	[ ]
Vendor Information	[ ]	Operating Procedure	[ ]	Electric Circuit Schedule	[ ]
OM Manual	[ ]	Operational Safety Requirement	[ ]	ICRS Procedure	[ ]
FSAR/SAR	[x]	IEFD Drawing	[ ]	Process Control Manual/Plan	[ ]
Safety Equipment List	[ ]	Cell Arrangement Drawing	[ ]	Process Flow Chart	[ ]
Radiation Work Permit	[ ]	Essential Material Specification	[ ]	Purchase Requisition	[ ]
Environmental Impact Statement	[ ]	Fac. Proc. Samp. Schedule	[ ]	Tickler File	[ ]
Environmental Report	[ ]	Inspection Plan	[ ]		[ ]
Environmental Permit	[ ]	Inventory Adjustment Request	[ ]		[ ]

20. Other Affected Documents: (NOTE: Documents listed below will not be revised by this ECN.) Signatures below indicate that the signing organization has been notified of other affected documents listed below.

Document Number/Revision	Document Number/Revision	Document Number Revision
HNF-SD-SNF-TI-015, rev 5		

21. Approvals

	Signature	Date		Signature	Date
Design Authority			Design Agent		
Cog. Eng. D. R. Duncan	*DRDuncan*	10/13/98	PE		
Cog. Mgr. J. R. Frederickson	*J.R.Frederickson*	10/13/98	QA		
QA D. W. Smith	*DWSmith*	10/13/98	Safety		
Safety R. P. Omberg	*RPComberg*	10/22/98	Design		
Environ.			Environ.		
Other J. P. Sloughter	*Ball for JP Sloughter per telcon*	10/22/98	Other		

DEPARTMENT OF ENERGY

Signature or a Control Number that tracks the Approval Signature

ADDITIONAL

K-Basins Particulate Water Content, and Behavior

D. R. Duncan, *M. G. Plys
DE&S Hanford, Richland, WA 99352
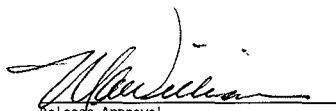U.S. Department of Energy Contract DE-AC06-96RL13200

Key Words: N-Reactor fuel, CVD process, particulate water content, characterization
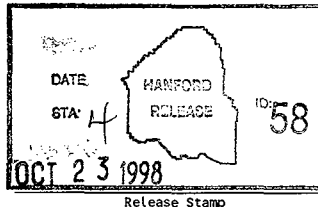
Abstract: This analysis summarizes the state of knowledge of K-basins spent nuclear fuel oxide (film, particulate or sludge) and its chemically bound water in order to estimate the associated multi-canister overpack (MCO) water inventory and to describe particulate dehydration behavior. This information can be used to evaluate the thermal and chemical history of an MCO and its contents during cold vacuum drying (CVD), shipping, and interim storage.

* Fauske & Associates

Release Approval   Date   Release Stamp

DATE   HANFORD
STA: H RELEASE   ID: 58
OCT 2 3 1998

Approved for Public Release

RECORD OF REVISION		(1) Document Number	
		HNF-1523	Page 1

(2) Title		
K-Basins Particulate Water Content, Behavior, and Impact		

CHANGE CONTROL RECORD

(3) Revision	(4) Description of Change - Replace, Add, and Delete Pages	Authorized for Release	
		(5) Cog. Engr.	(6) Cog. Mgr. Date
0	(7) Released by EDT #616191, 11/19/97	D. R. Duncan	J. R. Frederickson
1 RS	Complete document revision. The analysis, FAI/97-90 Rev. 4, attached to HNF-1523, Rev. 0 has been replaced by FAI/98-97 Rev. 3. This new analysis provides updated MCO water inventory estimates based on revised MCO particulate inventory estimates and eliminates follow-on calculations of MCO pressure and gas composition. The calculations of MCO pressure and gas composition can now be found in HNF-SD-TI-040.	D. R. Duncan 10/23/98	J. R. Frederickson 10/23/98

A-7320-005 (08/91) WEF168

FAI/98-97, Rev. 3

K-BASINS PARTICULATE WATER CONTENT,

BEHAVIOR, AND IMPACT

Submitted To:

Duke Engineering & Services Hanford, Inc.

2355 Stevens Drive

Richland, WA 99352

Prepared By:

Martin G. Plys

Fauske & Associates, Inc.

16W070 West 83rd Street

Burr Ridge, Illinois 60521

<u>Tel</u>: (630) 323-8750   <u>Fax</u>: (630) 986-5481

October 1998

TABLE OF CONTENTS

TABLE OF CONTENTS
(concluded)

LIST OF FIGURES

LIST OF TABLES

1.0 PURPOSE

The purpose of this work is to summarize the state of knowledge of K-basins spent nuclear fuel oxide (also called particulate or sludge) and its chemically bound water in order to estimate the associated multi-canister overpack (MCO) water inventory and to describe particulate dehydration behavior. This information can be used to evaluate the thermal and chemical history of an MCO and its contents during cold vacuum drying (CVD), shipping, and interim storage.

Low, nominal, and high MCO bound water content values after CVD are provided. A best-estimate law for uranium oxide hydrate thermal decomposition behavior is provided for prediction of water supply rate from this source during and after CVD.

This revision provides new MCO water inventory estimates based on revised MCO particulate inventory estimates [Sloughter, 1998], and eliminates follow-on calculations of MCO pressure and gas composition which are performed in more detail elsewhere [Plys, 1998]. Previous revisions (FAI/97-90, Rev. 4 and FAI/98-97, Rev. 1 and Rev. 2) contained a variety of information and calculations that were first-of-a-kind estimates or based on draft data, so some sections are omitted or revised using new information.

2.0 SUMMARY

Recent estimates of MCO particulate content (fuel oxide and hydrated fuel oxides) and recent experimental data on K-basins particulate dryout rates and physical properties are used here to estimate the range of expected MCO water content. Kinetic data for dehydration are refined for thermal modeling, but thermal decomposition is not credited here. MCO particulate content estimates, a source for this document, are largest for the case of an MCO with two scrap and three fuel baskets. For this case estimated values are 30 kg high, 6 kg nominal, and 1 kg low loaded at the K-basins [Sloughter, 1998] and excluding corrosion product generated after fuel cleaning.

Water inventory estimates, including generated particulate and free water sources, are (kg):

Scrap Baskets	High	Nominal	Low
Zero Scrap Baskets	4.52	1.30	0.26
One Scrap Basket	4.67	1.25	0.26
Two Scrap Baskets	4.84	1.21	0.26

The high water inventory is nearly independent of the number of scrap baskets because the $Al(OH)_3$ content is nearly constant. The nominal water inventory is about 1.25 kg and the low water content is about 1/4 kg in all cases. See Tables 5-1 and 5-2 for details.

The most significant contributor to the high MCO water estimate is an $Al(OH)_3$ film on cladding, whose water content lies between 3.3 and 3.7 kg. This film may not thermally decompose during either CVD, transport, or interim storage, so its water would only contribute to MCO pressurization by radiolysis. The next most significant high estimate contributors are adhering particulate for the case of two scrap baskets, about 1 kg water, and adhering particulate and canister particulate for the case of zero scrap baskets, about 0.3 and 0.24 kg water, respectively. But 92% of the high estimate canister particulate water is from Al and Fe hydrates that may not thermally decompose. Thus the case with the highest water inventory subject to

thermal decomposition is for two scrap baskets, where about 1.2 kg water from uranium oxide hydrates is the high value. Water borne by particulate generated after MCO loading is less than half of the 200 grams free water that may remain after CVD.

3.0 SOURCES AND UTILIZATION

Reference sources used to create technical bases and formulate assumptions are summarized here; detailed review of references is relegated to appendices where indicated. The meaning of reference data and their purpose for utilization are also discussed.

Sources are mentioned as follows: Section 3.1, MCO particulate inventory estimates which will be used to estimate the MCO water inventory; Section 3.2, a summary of water-bearing compounds of interest to MCO pressurization; Sections 3.3 to 3.11, details of these compounds; and Section 3.12, physical property data for particulate which are useful in understanding particulate composition.

3.1   MCO Particulate Inventory

Estimates of MCO particulate inventory are provided by [Sloughter, 1998]. The scope of the inventory includes material loaded into an MCO at K-basins that is literally not cladding and fuel in their original form. The term 'Particulate' is used because corrosion products become small, potentially entrainable particles. 'Sludge' is another term for existing K-basins corrosion products without specific regard to source, and this term is used in a variety of references sited herein. 'Canister particulate' refers to particulate found at the bottom of fuel canisters and within flow channels of a fuel assembly. The terms canister particulate and canister sludge are assumed synonymous in the report.

Table 3-1 contains the [Sloughter, 1998] inventory summary by source after fuel cleaning without further corrosion. Three estimates, high, nominal, and low, are supplied to illustrate the perceived range per particulate source. The cladding film consists of $Al(OH)_3$ for elements stored in closed aluminum canisters at K-West, visible as a thick white layer, and as a grey coating chiefly comprised of UO_44H_2O otherwise. Oxide layers exist on exposed metallic

Table 3-1: Summary of Derived Particulate Mass Values, kg/MCO								
Source	**Zero Scrap – Five Fuel Baskets**			**One Scrap – Four Fuel Baskets**			**Two Scrap – Three Fuel Baskets**		
	High	**Nominal**	**Low**	**High**	**Nominal**	**Low**	**High**	**Nominal**	**Low**
Aluminum Hydroxide Cladding Surface Film									
Scrap	0	0	0	1.54	0.39	0	3.08	0.77	0
Fuel	10.65	2.66	0	8.51	2.13	0	6.39	1.60	0
Uranium Peroxide Cladding Surface Film									
Scrap	0	0	0	0	0.05	0.07	0	0.10	0.14
Fuel	0	0.35	0.47	0	0.28	0.38	0	0.21	0.28
Oxide Film									
Scrap	0	0	0	0.45	0.05	0.03	0.9	0.1	0.06
Fuel	0.4	0.006	0.002	0.32	0.01	0.002	0.24	0.004	0.001
Adhering Particulate									
Scrap	0	0	0	7.80	0.78	0.23	15.60	1.56	0.47
Fuel	5.4	2.05	0.35	4.32	1.64	0.28	3.24	1.23	0.21
Canister Particulate	1.6	0.65	0	1.28	0.52	0	0.96	0.39	0
TOTAL	18.05	5.72	0.82	24.22	5.85	0.99	30.41	5.96	1.16
Rounded TOTAL	18	6	1	24	6	1	30	6	1

surfaces. Adhering Particulate listed in Table 3-1 consists of adhering and trapped particles found at fuel damage sites.

Particulate is generated after fuel cleaning due to corrosion in the basin, transfer to CVD, and at CVD before drainage and during the drying process itself. [Sloughter, 1998] provides a summary of post-cleaning particulate generation for a bounding MCO with two scrap baskets and a nominal MCO with one scrap basket. For a bounding MCO, 15 kg are estimated to be generated up to the time of MCO drainage, and 9.8 kg are estimated to be formed during CVD. For a nominal MCO, corresponding values are 0.075 kg and 0.309 kg.

Descriptions of the fuel loading process and fuel damage pertinent to the inventory are fully described in the reference and will not be repeated here.

3.2   Compounds of Interest

Compounds present in fuel coatings and particulate have been studied by [Sloughter and Barney, 1998]. Canister particulate TGA experiments by [Abrefah, 1998] and cladding film TGA data by [Marshman and Abrefah, 1997] provide further information. Direct observation or hypothesis yield these potential sources of water in an MCO:

$Al(OH)_3$, aluminum hydroxide, is found as a white or translucent film on cladding of fuel assemblies in some K-West aluminum canisters (which are sealed); it is not found on cladding in K-East canisters (which are open) or K-West steel canisters [summarized in Sloughter, 1998]. Some $Al(OH)_3$ may be present in particulate as well, comprising about 12% of canister particulate [Sloughter and Barney, 1998]. This compound can yield 1.5 moles H_2O per mole Al, about 35 weight percent.

$UO_3 \cdot xH_2O$, uranium trioxide hydrate, where $x=2$, schoepite, $x=0.85$ to 1.0, dehydrated schoepite, and possibly $x=0.5$ may either occur in uranium metal corrosion product [Danroc, 1982, and Taylor, et al., 1993] or may be formed by decomposition (see Appendix C references regarding the decomposition behavior

of UO_3 hydrates). $UO_2(OH)_2$ and $U_3O_8(OH)_2$ exist as compounds, but do not appear to be a priori present. Uranium oxides and hydroxides comprise the major fraction of canister particulate, about 72% [Sloughter and Barney, 1998].

$UO_4 \cdot xH_2O$, uranium peroxide hydrate, has been observed with $x=4$ as the primary constituent of a grey film on cladding [Marschman and Abrefah, 1997], and $x=2$ is its decomposition product [Sato, 1963].

$Fe(OH)_3$, iron hydroxide, and iron oxides, Fe_2O_3, hematite, and Fe_3O_4, magnetite, have been found in canister particulate [Sloughter and Barney, 1998]. These comprise about 13 weight percent of canister particulate.

Adsorbed water can potentially exist in multiple molecular layers fixed by hydrogen bonding to uranium oxide surfaces.

Free water can potentially remain in an MCO after cold vacuum drying, despite the fact that the purpose of cold vacuum drying is to remove this water and that pressurization tests exist to detect its presence. Hypothetical sources are: (1) Water contained in reentrant surface cavities, (2) Water which locally froze to ice during drying and did not thaw sufficiently for detection, (3) Water present in internal porosity of corrosion product, (4) Water retained between cladding and fuel whose escape is prevented by fuel corrosion product completely sealing off connected porosity, and (5) Water retained in cracks in fuel whose escape is similarly prevented.

Hypothetically, other compounds that exist in the K-basins could also be included in the MCO, such as hydrates present in concrete spallation products, constituents of resin beads which could evolve hydrocarbon gases, and biological sources which could evolve water and hydrocarbons. These are excluded from consideration based on assumptions of the particulate inventory panel [Sloughter, 1998].

References regarding these potential water sources are discussed subsequently.

3.3   Thermodynamic Data

Thermodynamic data for compounds of interest are summarized in Appendix A, and implications of these data are presented there as well. Thermodynamic data are used to make judgements regarding the potential for formation or decomposition of water-bearing compounds.

The most important implication from thermodynamic data is that formation of uranium trioxide hydrates is deemed practically impossible during cold vacuum drying steps after MCO drainage because of the relative values of partial pressures of water vapor (marginal), oxygen (too low), and hydrogen (too high). This conclusion applies to uranium peroxide hydrates too.

3.4   Aluminum Hydroxide Films

Films of Al(OH)$_3$ observed on cladding in closed K-West aluminum canisters have the potential to partially decompose during cold vacuum drying and interim storage based on evidence presented by [Sloughter and Barney, 1998]. In crystalline form, this compound is not expected to thermally decompose because temperatures greater than 100°C are required. However, amorphous Al(OH)$_3$ can partially decompose in vacuum near 50°C, although its decomposition in nitrogen occurs at about 100°C. PNNL TGA data for two samples (see Appendix B) suggest that thermal decomposition will begin at about 100°C, but it cannot be demonstrated that these samples represent the entire population. Thus while radiolytic decomposition probably is the only dominant physical process for evolution of water from Al(OH)$_3$, thermal decomposition cannot be definitively ignored at this time.

3.5   Uranium Trioxide Hydrate Formation

$UO_3 \cdot 2H_2O$ is formed under appropriate circumstances below temperatures between 80°C and 100°C, while $UO_3 \cdot 0.8H_2O$ is similarly formed at temperatures of 100°C and above [Danroc, 1982]. The circumstances required are simultaneous presence of nontrivial partial pressures of oxygen and water vapor, e.g., air saturated with water vapor at 60°C to 80°C or oxygen-saturated water [Danroc, 1982, and Taylor, et al., 1993]. Formation rate data presented in Appendix C show a maximum of 5% molar conversion of UO_2 to $UO_3 \cdot 2H_2O$ in 7 days at 60°C, when the initial UO_2 consists of finely divided, high specific area particles of about 0.2 micron diameter.

From references discussed in Appendix C, $UO_2(OH)_2$ and $U_3O_8(OH)_2$ are not expected to be significant.

In practice, UO_3 hydrates are simply not formed unless both water vapor and oxygen are present in substantial quantity, but there is no experimental quantification of a lower bound on oxygen concentration for the simple and expedient reason that conditions for formation of the hydrate in reasonable time are reported and ineffective conditions are avoided. As explained in Appendix A, conditions during CVD are at least ineffective, and probably prohibitive, for hydrate formation based on the literature. Formation rate data may be used to provide a conservative bound on water content via this mechanism.

3.6   Uranium Trioxide Hydrate Decomposition

$UO_3 \cdot 2H_2O$ decomposition rates depend upon both temperature and ambient water vapor partial pressure. Decomposition to $UO_3 \cdot H_2O$ has been observed under high vacuum at room temperature [Danroc, 1982] as described in Appendix D. However, the potential for decomposition must decrease with increasing water vapor pressure. PNNL experimental data of [Abrefah, et al., 1998] can be used for rate law derivation. As discussed in Appendix F, $UO_3 \cdot 2H_2O$ decomposition to $UO_3 \cdot H_2O$ appears to proceed with a first-order half-life of about 88 hours at the CVD temperature of 50°C and a steam pressure of about 100 mtorr (13 Pa). Thus much of this compound would remain in an MCO after CVD.

Loss of the remaining moles of water per mole of uranium appears to occur in two steps, first to either $UO_3 \cdot 0.8H_2O$ [Danroc, 1982] or to $UO_3 \cdot 0.5H_2O$ [Abrefah, et al., 1998], but the required temperatures exceed those planned for CVD. Thus these latter steps are expected to be significant only during storage at temperatures in excess of 50°C.

3.7 Uranium Peroxide Hydrate Formation

Uranium peroxide hydrate is typically formed by precipitation from uranium nitrate in nitric acid solution treated with hydrogen peroxide, as discussed in Appendix G. Obviously this condition does not exist at the K-basins, and a corrosion mechanism involving formation of aqueous uranium-bearing ions, their transport, and subsequent formation of insoluble compounds at or near cladding surfaces may be hypothesized to explain the observed surface cladding film. The role of radiolysis in this process is not quantified.

Since the precise mechanism for formation of the layer on cladding is unknown, the potential for formation of this compound elsewhere, such as on or inside corrosion product adhering to reactive metal or in spalled particles, is similarly unknown. Literature recipes for formation of UO_4 hydrates cannot be used to explain the presence or location of these compounds on fuel in the K-basins.

3.8 Uranium Peroxide Hydrate Decomposition

Uranium peroxide hydrate easily decomposes from $UO_4 \cdot 4H_2O$ to $UO_4 \cdot 2H_2O$ at room temperature in vacuum and between 50°C and 75°C at 4 mtorr as discussed in Appendix G. Loss of the remaining water is accompanied by reduction to UO3, but only at temperatures well in excess of those planned at CVD. Therefore, the ratio of moles water per mole uranium associated with this compound after CVD should be the same as that of undecomposed $UO_3 \cdot 2H_2O$. Decomposition data for uranium peroxide hydrate is used later to assign a post-CVD water content to corrosion product initially containing this compound.

3.9   Iron Hydrates

Iron hydrates discussed by [Sloughter and Barney, 1998] are not expected to decompose below 100°C, so any loaded inventory would survive CVD. Figure 3-1, reproduced from [Sloughter and Barney, 1998], illustrates the relationship between weight loss and a priori estimated Fe and Al hydroxide content in canister particulate. This information can be used to bound canister particulate water content.

3.10   Adsorbed Water

Adsorbed water can exist in layers of one or more molecules thick attached by hydrogen bonds to oxide surfaces. There are no data at present for adsorbed water on K-basins fuel. As shown in Appendix H, the quantity of adsorbed water potentially present in an MCO is negligible.

3.11   Free Water

There are no data taken with K-basins fuel for the amount of free water that could remain in an MCO after CVD. Sensitivity of results to this water source is discussed later, and indicates a project requirement that CVD remove free water effectively.

3.12   K-Basins Canister Particulate Physical Property Data

K-basins canister particulate physical property data for bulk density, particle density, water content, and uranium content are summarized in Appendix I. These data are used later to make inferences of the hydrate content of particulate which clings tenaciously to exposed fuel surfaces.

Figure 3-1:

Weight Loss Over the Temperature Ranges 100°C to 300°C Versus Percent Aluminum and Iron Hydroxides in Canister Particulate Samples From K-East and K-West Basin Canisters [Sloughter and Barney, 1998].
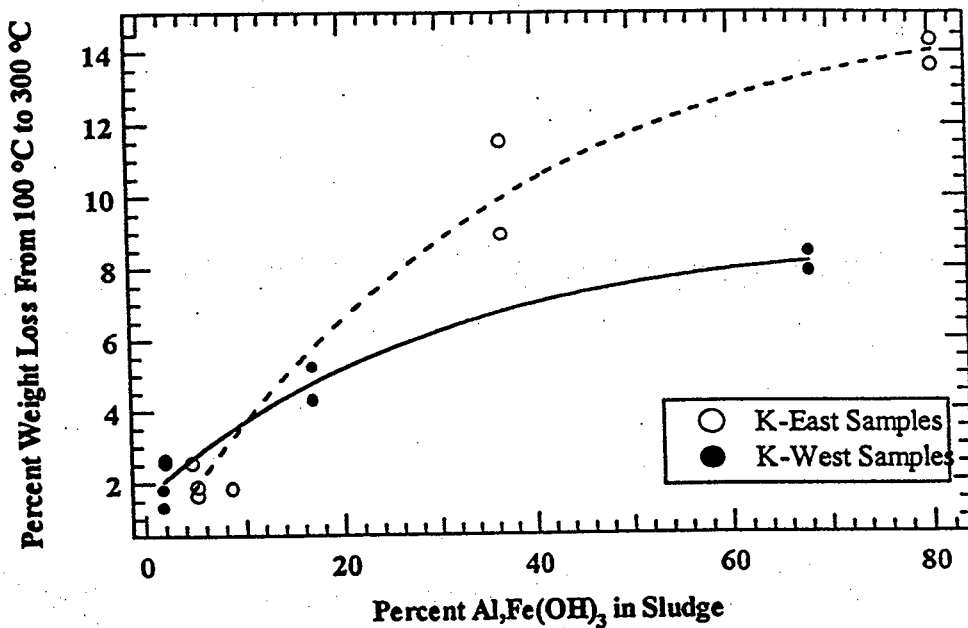
3.13 K-East Canister Particulate Dryout Data

Dryout data for K-East canister particulate may be used to estimate the water content of canister particulate deposits and adhering particulate. Table 3-2 summarizes weight loss ascribed to uranium oxide hydrates by [Abrefah, et al., 1998]. Their postulated decomposition steps are:

$$UO_3 2H_2O \rightarrow UO_3 \cdot H_2O$$

$$UO_3 \cdot H_2O \rightarrow UO_3 \cdot 0.5H_2O$$

$$UO_3 \cdot 0.5H_2O \rightarrow UO_3$$
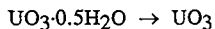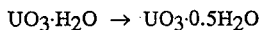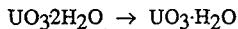
If a canister particulate sample contained only $UO_3 \cdot 2H_2O$, the maximum water fraction would be 11.1%. Data show that this canister particulate was only partially hydrated in general. An exceptional case is TGA #45 whose high water content is not explained by the decomposition model. The average water fraction, including TGA #45, is 7.4%.

Table 3-2:				
K-East Canister Particulate Hydrate Water Content Based on [Abrefah, et al., 1998].				
TGA Run	Mass (mg)			Weight (mg) at 425°C	% Weight Hydrate Water
	Peak 1	Peak 2	Peak 3		
40	16.38	8.19	8.19	988.04	3.3%
41	8.65	4.32	4.32	655.08	2.6%
42	17.36	8.7	8.66	604.64	5.7%
43	19.21	9.6	9.6	985.99	3.9%
44	17.51	8.75	8.75	324.89	10.8%
45	31.34	15.7	15.63	361.25	17.3%
46	17.94	9.0	8.93	442.39	8.1%

4.0 TECHNICAL BASES AND ASSUMPTIONS

Technical bases for MCO water content derived from experimental data and references are summarized here, and assumptions based on these references are listed and supported.

Technical bases formulated from the references are:

1. The particulate estimates of [Sloughter, 1998] comprise a detailed inventory and basis for identification of potentially water-bearing compounds.

2. Consistent with [Sloughter, 1998], high, nominal, and low values of MCO water content will be provided here corresponding to the three reference levels of particulate inventory. High values cannot credibly be exceeded for an entire MCO, although locally higher and lower values of underlying parameters could exist within an MCO. A nominal value is intended to represent a whole MCO on average, and a low value will occasionally characterize the contents of an MCO.

3. Uranium peroxide hydrates, if present as $UO_4 \cdot 4H_2O$ prior to CVD, will be decomposed during CVD to $UO_4 \cdot 2H_2O$, i.e., the water content associated with UO_4 hydrates cannot be greater than that associated with $UO_3 \cdot 2H_2O$. The technical basis is given in Appendix G.

4. K-East canister particulate dryout data [Abrefah, et al., 1998], described in Appendix E, provide a technical basis for particulate water content and drying behavior of UO_3 hydrates. These data are consistent with $UO_3 \cdot 2H_2O$ decomposition and average water contents below the theoretical value for this compound.

    Experimental data are interpreted for this work (see Appendix F) to imply: (1) The decomposition half-life range expected at 50°C is about 88 hours, (2) Loss of the first mole of water, i.e., decomposition to $UO_3 \cdot H_2O$, may partially occur under CVD conditions but is rate-limited and further decomposition cannot occur at CVD, and (3) A high water content corrosion product associated with reactive metal surfaces is given by that of $UO_3 \cdot 2H_2O$, or 11%, an average water content is 7.4% (see Section 3.13), and a low value is 3%.

One instance of a higher water content was seen, but: (a) it is not appropriate to apply this to a whole MCO, and (b) physically this implies the presence of $UO_4 \cdot 4H_2O$, which by the technical basis will decompose to have no greater water content than that of $UO_3 \cdot 2H_2O$.

5.   Conditions during CVD are either unfavorable or prohibitive to formation of uranium oxide hydrates after MCO water drainage, based upon consideration of equilibrium data (Appendix A). The water vapor partial pressure is high enough to theoretically allow formation of hydrates at the beginning of CVD, 100% relative humidity, and 50°C, but oxygen should be in insufficient abundance and hydrogen should be in excessive abundance to prohibit the reaction. After partial free water removal, the relative humidity will fall to low values and prohibit hydrate formation.

Further technical basis for this judgement is given by literature data on formation of uranium oxide hydrates and rate law data in Appendix C. For practical purposes, these hydrates are only formed in systems with high relative humidities and high oxygen content. Even in steam-air mixtures at 80°C and 80% relative humidity, less than 10% molar conversion of oxide to hydrate occurred over a 10 day period when the initial material was very fine (0.2 micron) uranium dioxide powder. It is not correct to assign non-negligible conversion rates to oxide films of much lower specific area for durations an order of magnitude shorter in systems with no obvious source of oxygen besides radiolysis, because radiolysis also liberates hydrogen that prevents hydrate formation (see Appendix A).

6.   Canister particulate may be assigned a high water content by assuming a composition of 80% Al + Fe hydrate at 30% water and the remainder $UO_3 2H_2O$. This is in accord with the largest Al + Fe compound mass fraction (see [Sloughter and Barney, 1998]) with equal weighting of the two elements and data presented in Appendix I. Note the resulting 26% water is in excess of the approximately 14% water for canister particulate with 80% Al + Fe shown in Figure 3-1. Further, the actual inventory of canister particulate presented by [Sloughter, 1998] was developed using a high density of 2.7 g/cm^3. But for derivation of a bounding water content, this value is physically too large. Because the highest bulk density of high water content canister particulate is 1.5 g/cm^3 (see Appendix I), canister particulate mass inventories may be reduced by the ratio $1.5 / 2.7 = 0.56$ for the purpose of calculating the bounding water content. Thus, the overall fractions of the [Sloughter, 1998] canister particulate inventory used for its bounding water content is 14.5%, rounded to 15%.

7.   About 200 g free water may remain in an MCO after CVD. See [Pajunen, 1998a and 1998b] for the technical basis.

Assumptions for MCO water inventory estimates are:

1. Adhering particulate (a category in the particulate inventory) is at most 50% mole fraction hydrated. This assumption is developed further in the calculations section, and stands as an assumption because there are no particulate density data for this category, only bulk density data.

    Associated data and equations are contained in Appendix I. Summarizing the logic of this assumption, the bulk density of this material exceeds the bulk density of K-East canister particulate samples, and the particle density associated with high bulk density K-East canister particulate exceeds the hydrate theoretical density. Therefore, this particulate can only be partially hydrated.

2. Thermal decomposition of $Al(OH)_3$ and $Fe(OH)_3$ will be negligible during CVD. This is supported by data for crystalline forms (see [Sloughter and Barney, 1998]) and is conservative for the present purpose. For $Al(OH)_3$, limited data shown in Appendix B also support this assumption.

3. Canister particulate may be assigned a nominal water content of 7.5% in accord with the data of Abrefah reported in Section 3.13. Because the relative proportion of water from U or Al + Fe hydrates is not known, a weighting of 75% from U hydrates and 25% from Al + Fe hydrates is chosen, corresponding to the 72% by weight of U compounds in this material cited by [Sloughter and Barney, 1998].

5.0 CALCULATIONS

5.1 Cladding Surface Films

Cladding surface film inventories from [Sloughter, 1998] employed a combination of aluminum hydroxide and uranium peroxide hydrate as follows: High, pure $Al(OH)_3$; Nominal, 25% $Al(OH)_3$, 75% UO_44H_2O; Low, pure UO_44H_2O. As described in Section 3, $Al(OH)_3$ may not thermally decompose at CVD, so a water content of 35% applies. UO_44H_2O will easily decompose to UO_42H_2O, so a water content of 11% applies.

5.2 Oxide Films on Scrap and Fuel

Oxide film masses of Table 3-1 were calculated assuming a density of 10 g/cc, equivalent to UO_2 at slightly less than theoretical density. As seen in Appendix I, the density of a hydrate is less than half that value, and the dominant hydrate expected to form based on Appendix C is $UO_3 \cdot 2H_2O$. Thus, the oxide mass may be multiplied by a factor of $0.5 * 0.11 = 0.055$ or 5.5% to yield a high water content for these contributions. This weight fraction also applies to any $UO_4 \cdot 4H_2O$, as discussed in Appendix G. Per the discussion in Appendix F, no credit is taken for decomposition of uranium oxide hydrates during CVD. A nominal water content is the average of Abrefah's data, about 7.5% [Abrefah, et al., 1998], again adjusted by a factor of 0.5 for the density, yielding a rounded value of 4%. Taking a low value of 3% similarly yields a low end water content of 1.5%.

5.3   Particulate on Scrap and Fuel

Particulate found on scrap and fuel listed in Table 3-1 is based upon measurements of the mass of particles that could be scraped and picked from metal fuel surfaces and underneath cladding adjacent to exposed surfaces, i.e., these particles tenaciously resisted handling and cleaning. Because the metal oxide tends to slough off after a thickness of about 3 microns is attained [Marschman, Pyecha, and Abrefah, 1997], and because the hydrate has an even lower density and should slough off too, and because of the high bulk density of tenacious particulate (Appendix I), it is assumed here that these particles are similar to the densest particles observed in canister particulate. From the data presented in Appendix I, a particle having the maximum observed particle density, 7.88 g/cc, if consisting of a mixture of hydrate at 5 g/cc and metal at 19 g/cc (a conservative combination) would have a hydrate mass fraction μ given by

$$\frac{1}{7.88} = \frac{\mu}{5} + \frac{1-\mu}{19} \tag{5-1}$$

resulting in $\mu = 50\%$. If instead a mixture of hydrate and oxide were postulated, then the hydrate content would only be 33%. Since there is no reason for metal to appear in the form of a particle firmly attached to the surface, and since metal particles would be reacted anyway, it is more reasonable to assume that the observed particles are mostly oxide. Given the high density of particles that could adhere to surfaces, it is clear that only a fraction of these particles can be hydrate. It is assumed that a hydrate fraction of 50% is a conservative upper bound.

Given 50% hydrate consisting of 11% water, 5.5% is assigned to the high water fraction for particulate found on fuel and scrap. The nominal and low water fraction values are found using Abrefah's data, as discussed for oxide film, and are numerically equal to those for oxide film, 4 and 1.5%, respectively.

5.4   Canister Particulate

Nominal values for canister particulate follow from mass fraction values cited by [Sloughter and Barney, 1998] and discussed in Section 3, namely, 12% $Al(OH)_3$, 13% $Fe(OH)_3$, and 75% uranium corrosion product by difference. While the water contents of $Al(OH)_3$ and $Fe(OH)_3$ are 35% and 25%, respectively, it is clear from Figure 3-1 that no more than about 7% water can be expected in canister particulate with a 25% Al + Fe content. A water content of 7.5% may be used for canister particulate to be consistent with the average of Abrefah's data cited above, and with no density correction needed. Since the data do not provide a means to partition water among U and Al + Fe (note 25% Al + Fe hydrates yields 7.5% H_2O), 25% is assumed from Al + Fe and 75% from U.

High values are obtained by noting weight loss data of Figure 3-1 and composition data presented in Appendix I, which show that canister particulate may contain more aluminum and iron compounds than uranium compounds. But water loss below 100°C and above 300°C are not included in the data, and 80% Al + Fe hydrate implies 24% water. Adding 20% uranium hydrate at 11% water yields a high water content of 26%. As noted in Appendix I, the highest bulk density of high water content canister sludge is 1.5 g/cm^3. However, [Sloughter, 1998] calculated the amount of canister particulate using a density of 2.7 g/cm^3. It is not appropriate to combine a high water content with a high bulk density, as already discussed with regard to oxide films in Section 5.2. Canister particulate with a high water content must have a low density, so that the bounding canister particulate inventory from Table 3-1 should be reduced by a factor of at least 1.5 / 2.7 = 0.56 prior to calculation of water inventory. Therefore an overall factor of (26%) (0.56) = 14.5%, or 15% when rounded, may be used to calculate the bounding water content of canister particulate from the reference particulate mass values listed in Table 3-1. Note that the uranium compound mass fraction is 20%, but the fraction of water from uranium compounds is 2% / 26% = 0.077, or about 8%.

A low value of 2% water fraction is selected from Figure 3-1 and ascribed entirely to uranium oxide hydrates.

5.5   Generated Particulate

As noted in Section 3.1, a bounding value for generated particulate through the end of CVD is about 25 kg. However, as discussed in Appendix A, hydrate formation cannot occur when oxygen is absent and hydrogen is present, as would be the case after MCO drainage. Therefore, a high value of water content from generated particulate need only consider particulate generated up to the time of MCO drainage, for which a bounding value of 15 kg and a nominal value of 0.075 kg apply.

Considering 60°C rate data in Appendix C to bound conversion of oxide to hydrate, a conversion fraction of 5% is appropriate. Because the hydrate water fraction is 11%, the overall high water fraction for generated particulate is 0.55%. When applied to the 15 kg bounding generated particulate mass, this results in only 0.083 kg water, and the nominal generated particulate mass would bear less than 1 gram water.

Thus, water chemically bound to generated particulate may be neglected for all but the high particulate cases. Bounding areas used by [Sloughter, 1998] are 4.5 m^2 per scrap basket and 0.79 m^2 per fuel basket, so an area ratio may be applied to the 15 kg generated particulate mass calculated for two scrap and three fuel baskets to yield high values with one and zero scrap baskets. These area ratios are 0.64 and 0.35, respectively. For an MCO with one scrap basket, 9.6 kg of generated particulate would bear 0.053 kg water. For an MCO with no scrap basket, 5.25 kg generated particulate would bear 0.029 kg water.

5.6   Summary of Water Inventory

Table 5-1 contains a summary of the MCO particulate water inventory based on line-item particulate sources from Table 3-1, and Table 5-2 contains a similar summary based on compound source. In all cases, 200 grams free water are considered because this amount may remain when an MCO is declared dry.

Table 5-1: Summary of Water Content Values, kg/MCO

Source	Zero Scrap - Five Fuel Baskets			One Scrap - Four Fuel Baskets			Two Scrap - Three Fuel Baskets		
	High	Nominal	Low	High	Nominal	Low	High	Nominal	Low
Cladding Film									
Al Film Mass (1)	10.65	2.66	0	10.05	2.52	0	9.47	2.37	0
Al Water Mass	3.728	0.931	0	3.518	0.882	0	3.315	0.830	0
U Film Mass (2)	0	0.35	0.47	0	0.33	0.45	0	0.31	0.42
U Water Mass	0	0.038	0.052	0	0.036	0.050	0	0.034	0.046
Oxide Film									
Oxide Mass	0.4	0.006	0.002	0.77	0.06	0.032	1.14	0.104	0.061
Water %	5.5%	4%	1.5%	5.5%	4%	1.5%	5.5%	4%	1.5%
Water Mass	0.022	<0.001	<0.001	0.042	0.002	<0.001	0.063	0.004	0.001
Adhering Particulate									
Oxide Mass	5.4	2.05	0.35	12.12	2.42	0.51	18.84	2.79	0.68
Water %	5.5%	4%	1.5%	5.5%	4%	1.5%	5.5%	4%	1.5%
Water Mass	0.297	0.082	0.005	0.667	0.097	0.008	1.036	0.112	0.010
Canister Particulate									
Oxide Mass	1.6	0.65	0	1.28	0.52	0	0.96	0.39	0
Water %	15%	7.5%	2%	15%	7.5%	2%	15%	7.5%	2%
Water Mass	0.24	0.049	0	0.192	0.039	0	0.144	0.029	0
Generated Particulate Water (3)	0.029	0	0	0.053	0	0	0.083	0	0
Free Water	0.2	0.2	0.2	0.2	0.2	0.2	0.2	0.2	0.2
TOTAL Water Mass	4.516	1.301	0.257	4.672	1.256	0.258	4.837	1.209	0.256

(1) Always 35% H_2O.   (2) Always 11% H_2O.   (3) 0.55% of generated particulate at MCO drainage.

Table 5-2: Post-CVD Particulate Water Content Summary (kg)

Source		High	Nominal	Low
Zero Scrap, Five Fuel				
Al(OH)$_3$	(1)	3.728	0.931	0
Uranium Oxide Hydrates	(2)	0.367	0.158	0.057
Al+Fe Hydrates	(3)	0.221	0.012	0
Free		0.2	0.2	0.2
TOTAL		4.516	1.301	0.257
One Scrap, Four Fuel				
Al(OH)$_3$	(1)	3.518	0.882	0
Uranium Oxide Hydrates	(2)	0.777	0.164	0.058
Al+Fe Hydrates	(3)	0.177	0.01	0
Free		0.2	0.2	0.2
TOTAL		4.672	1.256	0.258
Two Scrap, Three Fuel				
Al(OH)$_3$	(1)	3.315	0.830	0
Uranium Oxide Hydrates	(2)	1.189	0.172	0.056
Al+Fe Hydrates	(3)	0.133	0.007	0
Free		0.2	0.2	0.2
TOTAL		4.837	1.209	0.256

(1)   Cladding Film; High=100% from Al(OH)$_3$, Nominal=51% from Al(OH)$_3$, and Low=0% from Al(OH)$_3$.

(2)   Cladding Film, Oxide Film, Adhering Particulate, and Canister Particulate.

(3)   Canister Particulate; High=92% from Al+Fe hydrates, Nominal=25% from Al+Fe hydrates.

6.0 REFERENCES

J. Abrefah, H. C. Buchanan, and S. C. Marschman, "Drying Behavior of K-East Canister Sludge," PNNL-11628, UC-602, Pacific Northwest National Laboratory, Richland, WA, May 1998.

J. Danroc, "Evolution Superficielle et Aptitude au Compactage des Poudres de Dioxyde d'Uranium," Doctoral Thesis, l'Institut National Polytechnique de Grenoble, April 1982.

Duncan, D.R., and Ball, D.E., "Thermal Analysis of Cold Vacuum Drying of Spent Nuclear Fuel," HNF-SD-SNF-CN-023, Rev. 0, DE&S Hanford, Richland, WA, 1997.

Garvin, L.J., "Canister Storage Building Safety Analysis Report," HNF-SD-SNF-RPT-044, Rev. 7, May 1997.

J. Irwin, "Cold Vacuum Drying Facility Design Requirements," HNF-SD-SNF-DRD-002, Rev. 1, Numatech Hanford Company, September 1997.

Marschman, S.C., and Abrefah, J., "Highlight Report: Water Content of Film Coatings on K-East Fuel Surfaces," SNFCT97:040:R00, March 1997.

Marschman, S.C., Pyecha, and Abrefah, J., "Metallographic Examination of Damaged N Reactor Spent Nuclear Fuel Element SFEC5.4378," PNNL-11438, UC-602, August 1997.

Plys, M.G., et al., "Hanford Spent Nuclear Fuel Safety Analysis Model: User's Manual," FAI/97-36, Rev. 1, Fauske & Associates, Inc., Burr Ridge, Illinois, 1997.

T. Sato, "Preparation of Uranium Peroxide Hydrates," J. Appl. Chem., Vol. 13, August 1963, pp. 361-365.

J.P. Sloughter, "Estimates of Particulate Mass in Multi-Canister Overpacks," HNF-1527, Rev. 2, Numatec Hanford Corporation, Richland, WA, October 1998.

Sloughter, J.P., and Barney, G.S., "Identities of Compounds in Spent Nuclear Fuel Coatings and Particulates Sealed in Multi-Canister Overpacks," HNF-2667, Rev. 1 (Draft), Numatec Hanford Corporation, Richland, WA, July 1998.

P. Taylor, R. J. LeMire, and D. W. Wood, "The Influence of Moisture on Air Oxidation of UO_2: Calculations and Observations," Nucl. Tech., Vol. 42, Nov. 1993, pp. 164-170.

APPENDIX A

THERMODYNAMIC DATA AND IMPLICATIONS

A.1   Purpose and Summary

The purpose of this Appendix is to conveniently summarize thermodynamic data for species of concern to the MCO water inventory, and use these data to describe limitations on the formation and decomposition of hydrates for conditions pertinent to the K-basins, cold vacuum drying, and dry storage.

The equilibrium vapor pressure curve for decomposition of $UO_3 \cdot 2H_2O$ is very close to that of water vapor over water. The hydrogen pressure to prevent hydrate formation is orders of magnitude less than the oxygen pressures needed for formation, indicating that radiolysis of water vapor would prohibit formation.

The hydrogen partial pressure is actually determined by competing rates: Formation by oxidation of reactive uranium surfaces by water, and removal by convection. Evaluation of the hydrogen partial pressure is a moot point because any result must be many of orders of magnitude greater than the equilibrium value to prevent hydrate formation.

Uranium hydrates can only form in an MCO when reactive surface area is present, so the presence of oxide as a precursor to hydrate is perfectly correlated with the presence of reactive metal for oxidation by water vapor.

During cold vacuum drying, if there is a reactive metal surface present, uranium dioxide will form and this material in turn could potentially be converted into hydrate. However, the local partial pressure of hydrogen gas is always sufficient to prevent this reaction.

Therefore, UO_3 hydrates cannot form in an MCO during cold vacuum drying after removal of the oxygen initially present.

The presence of hydrogen similarly prevents formation of other UO_3 hydrates. As shown in Appendix C, these other hydrates simply do not form unless the local temperature is close to about 100°C anyway, and at CVD temperatures only $UO_3 \cdot 2H_2O$ would be observed as a reaction product.

Insufficient thermodynamic data exist on the UO_4 hydrates for conclusions to be drawn on this basis alone, and literature concerning observed formation and decomposition is summarized in Appendix G.

A.2 Uranium Oxide Hydrate Thermodynamic Data

Thermodynamic data are taken from JANAF [Chase, et al., 1985], [Katz, Seaborg, and Morss, 1986], [Taylor, et al., 1993], and [O'Hare, et al., 1988]. Table A-1 summarizes these data and includes estimates for $UO_3 \cdot 0.8H_2O$. Multiple data sources for the same compound are included so that values may be compared. We deduce that $UO_3 \cdot H_2O$ from [Katz, Seaborg, and Morss, 1986] corresponds to β - $UO_2(OH)_2$ from [Taylor, et al., 1993], and that values for $UO_3 \cdot 2H_2O$ are in accord between these two references. The heat of formation for $UO_3 \cdot 0.8H_2O$ was deduced by noting a linear variation in this parameter with water content, and its entropy of formation was deduced similarly.

Sufficient data exists to construct equilibrium decomposition curves for the $UO_3 \cdot xH_2O$ family. These are presented here as Figure A-1 [Plys, 1997]. Entropy data are lacking for $UO_4 \cdot xH_2O$ compounds, but [Cordfunke, 1978] and [O'Hare, et al., 1988] provide the following vapor pressure curve:

$$UO_4 \cdot 4H_2O \ \rightarrow \ UO_4 \cdot 2H_2O + 2H_2O$$
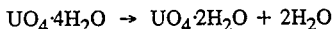
$$\ell og_{10}(P) \ = \ 8.055 - \frac{3056}{T} \tag{A-1}$$

where P is in atmospheres.

Table A-1: Thermodynamic Data Comparison. Values in parentheses are derived.						
Compound	ΔH_f kJ/mol	s J/mol	c_p J/mol·K	ΔS_f J/mol·K	ΔG_f kJ/mol	Ref.
H_2	0	130.68	28.836	0	0	2
O_2	0	205.15	29.38	0	0	2
U	0	50.2	27.66	0	0	1
$H_2O(g)$	-241.83	188.83	33.59	(-44.43)	-228.58	2
$H_2O(\ell)$	-285.83	69.95	75.35	(-163.31)	-237.14	2
UO_2	-1085.0	77.03	63.60		-1031.8	1
UO_3	-1223.8	96.11	81.7	(-261.8)	(-1145.8)	1
UO_3		96.11	81.7		-1145.7	3
$UO_3 \cdot H_2O$	-1533	134		(-457.2)	-1397	1
$\beta - UO_2(OH)_2$	(-1534)	138	141	(-453.2)	-1398.7	3
$UO_3 \cdot 2H_2O$	-1827	176				1
$UO_3 \cdot 2H_2O$	(-1826)	188.54	172	(-635.9)	-1636.5	3
$UO_3 \cdot 0.9H_2O$	(-1506.3)	126	140	(-441.9)	-1374.6	3
$UO_3 \cdot 0.85H_2O$	-1492					1
$UO_3 \cdot 0.8H_2O$	(-1477)	(120)	(140)			
$UO_3 \cdot 0.85H_2O$	-1491.4	123			-1362.3	4
$UO_3 \cdot 0.6H_2O$	-1424.6	118			-1308.1	4
$UO_4 \cdot 2H_2O$	-1782					1
$UO_4 \cdot 4H_2O$	-2384					1

References:

1. Katz, Seaborg, & Morss, 1986.
2. Chase, et al., 1985.
3. Taylor, et al., 1993.
4. O'Hare, et al., 1988.

Figure A-1: Equilibrium Decomposition Curves for the $UO_3 \cdot xH_2O$ Family.

VAPOR PRESSURE CURVES USING BOUNDING ENTROPY VALUES ARE RECOMMENDED
TO PRESERVE THE TRANSITIVE NATURE OF THE CURVES WITH STOICHIOMETRY NUMBER

Ln(P) = A + B/T yields:

		A	B	note P in atm!
UO3.2H2O	to UO3.H2O:	15.912	-6131	
UO3.H2O	to UO3.0.5H2O:	18.382	-7766	
UO3.0.5H2O	to UO3:	18.408	-8488	

UO3.xH2O Decomposition P(H2O)

- 2.0 → 1.0
- 1.0 → 0.5
... 0.5 → 0.0
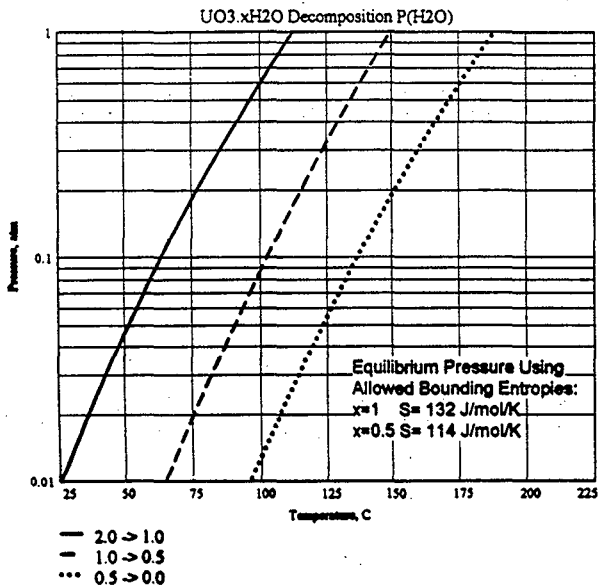
A.3 UO3 Hydrate Thermodynamic Data Implications

The fact that some oxygen must be present to allow formation of UO_3 hydrates is evident from the negative free energy change for a reaction with oxygen present and the positive free energy change for a reaction with oxygen absent:

$$UO_2 + \tfrac{1}{2}O_2 + 2H_2O \rightarrow UO_3 \cdot 2H_2O, \quad \Delta G = -147.5 \text{ kJ/mol}$$

$$UO_2 + 3H_2O \rightarrow UO_3 \cdot 2H_2O + H2, \quad \Delta G = +81 \text{ kJ/mol}$$
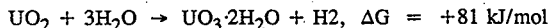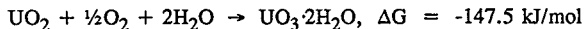
The implication of these equations is that there is some equilibrium oxygen concentration at which hydrate formation becomes thermodynamically permissible.

For the first reaction above,

$$k_1 = e^{-\Delta G/RT} = \left[p^2 (H_2O) \, p^{1/2} (O_2) \right]^{-1} \tag{A-2}$$

at 25°C, yields $k_1 = 7.17 \times 10^{25}$ and setting $p(H_2O) = 0.03$ atm, the saturation value, yields $p(O_2) = 4 \times 10^{-12}$ atm.

But the second reaction yields the hydrogen pressure required to prohibit formation of the hydrate:

$$k_2 = \frac{p(H_2)}{p^3(H_2O)} \tag{A-3}$$

At 25°C $k_2 = 6.3 \times 10^{-15}$, so with $p(H_2O) = 0.03$ atm, $p(H_2) = 1.7 \times 10^{-19}$ atm.

The hydrogen partial pressure to prevent hydrate formation is so low that it is absolutely clear that the threshold is exceeded when uranium is locally reacting with water to form hydrogen.

A.4   References

M. W. Chase, et al., "JANAF Thermochemical Tables," Third Edition, J. Phys. Ref. Data, Vol. 14, 1985, Supplement 1.

E. H. P. Cordfunke, "The Chemical Thermodynamics of Actinide Elements and Compounds, Part 3: Miscellaneous Actinide Compounds," IAEA, Vienna, 1978.

J. J. Katz, G. T. Seaborg, and L. R. Morss, "The Chemistry of the Actinide Elements," Second Edition, Chapman and Hall, New York, 1986.

P. A. G. O'Hare, B. M. Lewis, and S. N. Nguyen, "Thermochemistry of Uranium Compounds XVII: Standard Molar Enthalpy of Formation at 298.15 K of Dehydrated Schoepite $UO_3 \cdot 0.9H_2O$," Thermodynamics of (schoepite + dehydrated schoepite + water), J. Chem. Thermodynamics, 1988, Vol. 20, pp.1287-1296.

M. Plys, FAI Memorandum to J. Abrefah (PNNL), and D. Duncan and J. Swenson (DE&SH), "Hydrate Decomposition Vapor Pressures, dated August 26, 1997.

P. Taylor, R. J. LeMire, and D. W. Wood, "The Influence of Moisture on Air Oxidation of UO_2: Calculations and Observations," Nucl. Tech., Vol. 42, Nov. 1993, pp. 164-170.

APPENDIX B

THERMO-GRAVIMETRIC ANALYSIS OF Al(OH)$_3$ COATING

Figures B-1 and B-2 contain thermo-gravimetric analysis drying results from coating sample CS-4 which consists predominately of Al(OH)$_3$. These data are taken from the reference below and presented here because they are not yet available in final published form. These data were taken by PNNL in the 325 Building laboratories.

Reference

B. J. Makenas to R. P. Omberg, "Data from the Analysis of Cladding Coatings and Internal Sludge," DE&S Hanford Internal Memorandum, dated April 20, 1998.

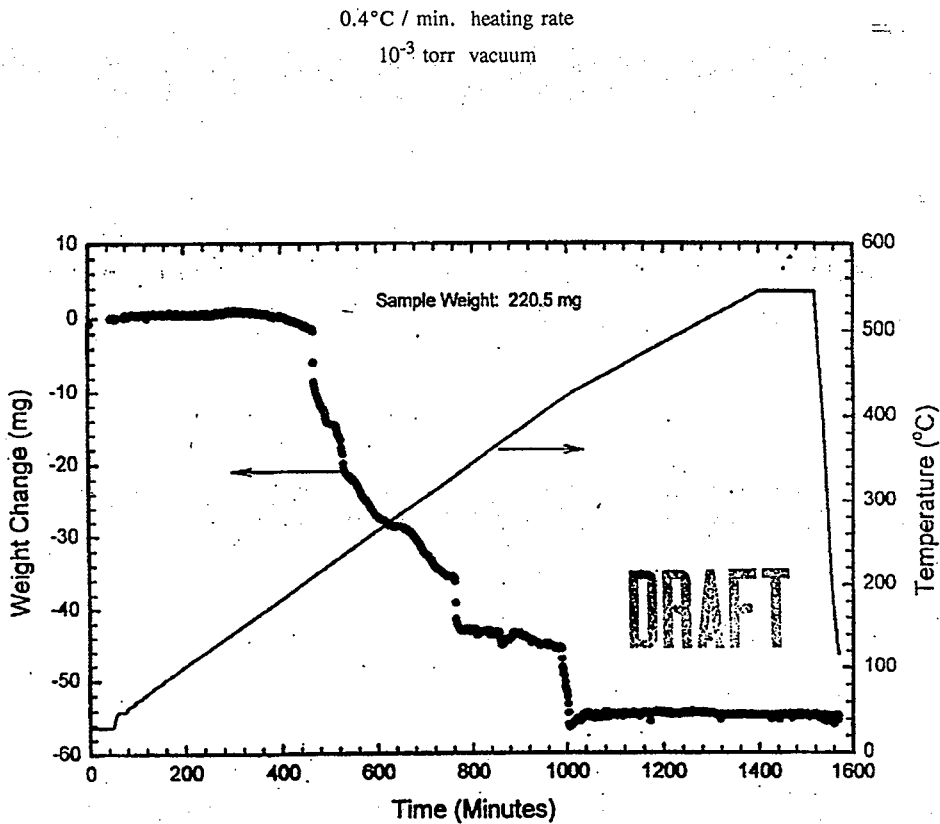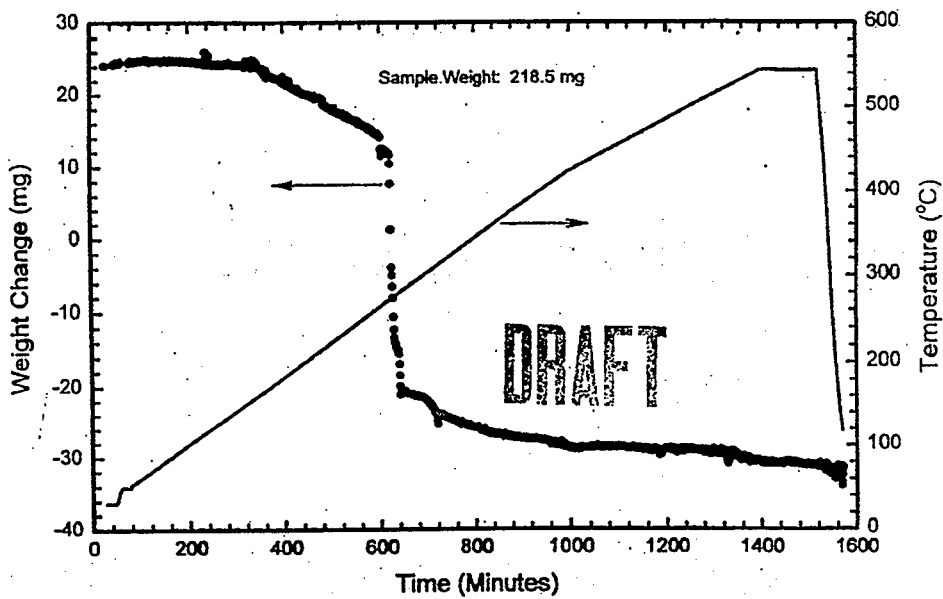**Figure B-1: Thermo-Gravimetric Analysis Drying Results from Coating Sample CS-4.**

0.4°C / min. heating rate

10^{-3} torr vacuum

Figure B-2: Duplicate Thermo-Gravimetric Analysis Drying Data from Coating Sample CS-4.

0.4°C / min. heating rate

10^{-3} torr vacuum

APPENDIX C

URANIUM TRIOXIDE HYDRATE FORMATION

C.1 Purpose and Summary

The purpose of this Appendix is to summarize literature data regarding the conditions and rates of formation of UO_3 hydrates, principally $UO_3 \cdot 2H_2O$. Literature regarding formation agree universally that either oxygenated water or steam-air environments are required.

C.2 Formation Conditions

Literature discussing the formation of UO_3 hydrates universally describes the required conditions as either oxygenated water or steam/air environments. [Taylor, et al., 1993] writes:

> *"The formation of DS [Dehydrated schoepite, $UO_3 \cdot 0.9H_2O$] by oxidation of UO_2 in oxygenated water at temperatures from 87°C to 177°C was first reported by Aronson. More recent studies have confirmed that this phase is a common oxidation product on unused UO_2 fuel oxidized in either aerated water or aerated steam (above ~50% steam saturation) at temperatures near 200°C ... "*

Taylor, et al., also describe experience with long-term (on order years) formation of $UO_3 \cdot 2H_2O$ during storage in laboratory air and air-saturated water at room temperature.

Observations of [Danroc, 1982] are consistent with Taylor, et al.'s discussion and references. Danroc used UO_2 powders of submicron size, about 0.2 micron diameter, and found that exposure to steam-air mixtures of 80% relative humidity at 60°C and 80°C resulted in partial conversion of the powder to $UO_3 \cdot 2H_2O$ during the course of a number of days. At 100°C, his hydrate product was $UO_3 \cdot 0.85H_2O$.

UO_3 hydrates are also commonly formed by exposing anhydrous UO_3 to liquid or vapor water as exemplified by the work and references of [Hoekstra and Siegel, 1973].

C.3   Formation Rate

The only available formation rate data are those of Danroc, and his low-temperature data are summarized in Figure C-1. It is seen that formation is faster at the higher temperature, but after 10 days the molar conversion is only about 8%. During the portion of cold vacuum drying (CVD) with high relative humidity and a nominal operating temperature of 50°C, conditions are closer to those of the 60°C data, and less than 5% conversion on a molar basis would be expected for durations on the order of only a day. As mentioned above, Danroc's data were taken with finely divided 0.2 micron UO_2 powder, so formation of hydrates should take place even more slowly during CVD.

[Katz and Rabinowitch, 1951] mention existence of Manhattan project data on rates of hydration, but provide no quantitative information.

C.4   Other Uranium Oxide Hydrates

Two other uranium oxide hydrates, β-$UO_2(OH)_2$ and $U_3O_8(OH)_2$, are discussed by [Taylor, et al., 1993] and [Hoekstra and Siegel, 1973]. These apparently do not form directly from UO_2, but either from hydration of UO_3 or decomposition of $UO_3 \cdot 2H_2O$. According to [Taylor, et al., 1993],

> *"Although the calculated stability relationships indicate narrow stability fields for both β-$UO_2(OH)_2$ and $U_3O_8(OH)_2$, neither of these phases has been observed as an oxidation product on UO_2, nor as a natural mineral. The compound β-$UO_2(OH)_2$ can be synthesized by contacting water with UO_3 or $UO_3 2H_2O$ at 200°C to 290°C in a sealed vessel, whereas [UO_3 0.9H_2O] is formed at 80°C to 200°C."*

Figure C-1: Danroc's $UO_3 \cdot 2H_2O$ Formation Data:
Aging of Submicron UO_2 Powder in Humid Air.

UO3.2H2O Formation from UO2 - J. Danroc

Aging 60 C 80% Humidity
Aging 80 C 80% Humidity
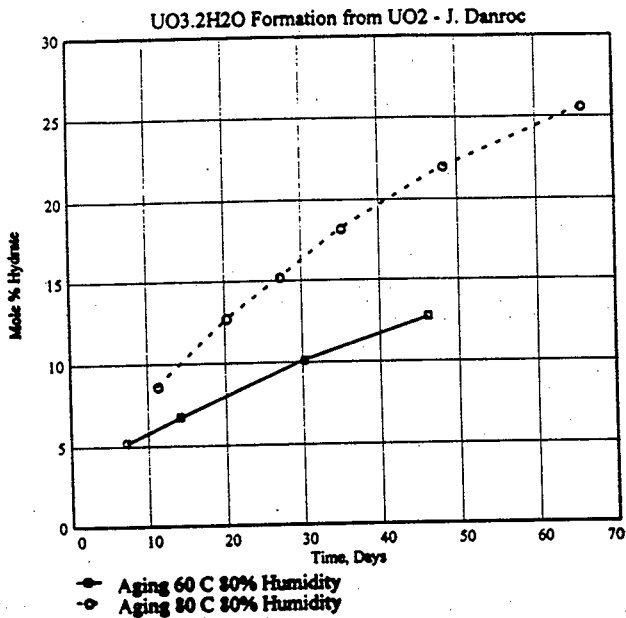
These compounds need not be considered for estimation of bounding water content because $UO_3 \cdot 2H_2O$ has about twice the water.

C.5   References

J. Danroc, "Evolution Superficielle et Aptitude au Compactage des Poudres de Dioxyde d'Uranium," Doctoral Thesis, l'Institut National Polytechnique de Grenoble, April 1982.

H. R. Hoekstra and S. Siegel, "The Uranium Trioxide-Water System," J. Inorg. Nucl. Chem., Vol. 35, pp. 761-779, Pergamon Press, UK, 1973.

Joseph J. Katz and Eugene Rabinowitch, "The Chemistry of Uranium: The Element, Its Binary and Related Compounds," National Nuclear Energy Series, Manhattan Project Technical Section, Division VIII - Volume 5, Dover Publications, New York, 1951.

P. Taylor, R. J. LeMire, and D. W. Wood, "The Influence of Moisture on Air Oxidation of UO_2: Calculations and Observations," Nucl. Tech., Vol. 42, Nov. 1993, pp. 164-170.

APPENDIX D

URANIUM TRIOXIDE HYDRATE DECOMPOSITION

D.1 Purpose and Summary

The purpose of this Appendix is to summarize literature data on the decomposition of uranium oxide hydrates, chiefly $UO_3 \cdot 2H_2O$ and its decomposition products with $x < 2$, where x is the water stoichiometry number.

Literature data for $UO_3 \cdot xH_2O$ decomposition may be summarized as:

1. Loss of the first mole of H_2O from $UO_3 \cdot 2H_2O$ depends strongly upon the ambient water vapor pressure and is in accord with equilibrium data.

2. Loss of the first mole of H_2O from $UO_3 \cdot 2H_2O$ is expected to occur in about 100 hours at 75°C given a water vapor pressure low enough, presumably below 1 kPa.

3. Loss of the remaining water requires temperatures well above 100°C and a kinetic rate law is required to quantify the time; the ambient water vapor pressure should not matter so long as it is well below the equilibrium for decomposition.

D.2 Literature Data [Hoekstra and Siegel, 1973]

The most comprehensive study of $UO_3 \cdot xH_2O$ decomposition routes is probably that of [Hoekstra and Siegel, 1973]. These authors summarize previous references and conclude that $UO_3 \cdot 2H_2O$ tends to decompose to $UO_3 \cdot 0.8H_2O$. Unfortunately, this is not always true because the data of [Danroc, 1982] clearly show intermediate formation of $UO_3 \cdot H_2O$. Note that the hydrates are written here as $UO_3 \cdot xH_2O$, but in references like Hoekstra and Siegel care is taken to identify the precise structures, for example $UO_2(OH)_2$ is a more proper way to express the monohydrate. For our purposes here the actual structures require no discussion, and the impact

of the structures is directly addressed by the choice of thermodynamic data and by the real, observed decomposition behavior that will be captured by equilibrium and kinetic models.

Danroc provides decomposition histories for four samples at 25°C and vacuum that can be used for the first phase of $UO_3 \cdot 2H_2O$ decomposition. Danroc also provides histories for two heatup rates, 4°C/hr and 5°C/min, from 25°C to 400°C that can be used for the loss of remaining water. Danroc's decomposition data are shown in Figure D-1.

The first portion of the data indicates time in hours under vacuum of 10^{-5} torr or about 10^{-3} Pa at 25°C for four samples treated for 0, 20, 35, and 66 days in humid air at 80°C. Note from Figure D-1 that Danroc's samples were only partially hydrated. The extent of hydration increased with treatment time (see Appendix C). Danroc believed the hydrate existed as a layer surrounding an oxide nucleus.

The second portion of the data is for temperatures above 25°C. Here there are four pairs of curves where the dashed line corresponds to heating at a slow rate, 4°C/hour, and the solid line corresponds to heating at a rapid rate, 5°C/minute. Danroc's particle sizes were very small, about 0.2 μm, so the combination of very low pressure and very small particles makes it difficult to directly apply his results for K-basins sludge.

[Katz and Rabinowitch, 1951] reference a Columbia study and provide a data table for loss of the first mole of water from $UO_3 \cdot 2H_2O$ at four temperatures, 61°C, 77°C, 100°C, and 118°C in water vapor of unknown partial pressure, and one point in vacuum at 28°C. Columbia data were mistakenly quoted by Katz and Rabinowitch in terms of minutes, but the correct durations are in hours:

Time Required for $UO_3 \cdot 2H_2O$ Decomposition to $UO_3 \cdot H_2O$, hours.						
Sample	Vacuum	61°C	77°C	87°C	100°C	118°C
From UO_3	-	> 518	< 95	> 12	< 2	< 1
From UO_4	< 123	> 100	< 122 > 48	< 2	-	-

Figure D-1:   French $UO_3 \cdot xH_2O$ Decomposition Data [Danroc, 1982].
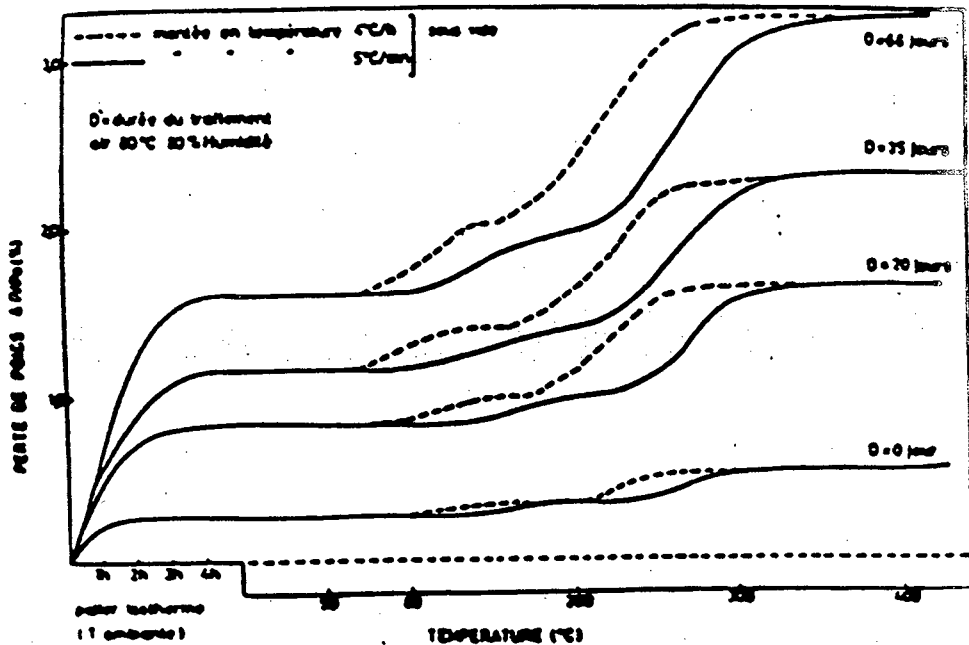
These data at 77°C are in accord with PNNL data for K-basins sludge to be discussed below, wherein a half-life for decomposition at 75°C is about 40 hours. These data are consistent with the following interpretation: below about 100°C, the water vapor partial pressure is very important in determining the rate of decomposition, and above 100°C for water vapor pressures well below 1 atm, this effect is not important. This interpretation follows from the observation of greater than 518 hours for decomposition at 61°C -- whereas Danroc observed complete decomposition in less than 240 minutes at 25°C under vacuum; this interpretation is also expected from thermodynamic data.

[Huttig and von Schroeder, 1922], also cited in [Katz and Rabinowitch, 1951] provide a data table for loss of water under about 15 torr water partial pressure, or 2 kPa, and for temperatures up to 450°C. Here one sample was heated and examined after various temperatures were attained, but the heating schedule is not stated, and several data points were taken at 100°C but the dwell time was not indicated. It is not clear why several points were taken at 100°C although this was probably done because the decomposition was observed (or anticipated) to be more rapid. Their data provide an illusion of congruent decomposition at that temperature which is contradicted by all other sources. Also the decomposition time at 100°C is at least 40 minutes (and probably on the order of an hour) if the UO_4 heatup schedule in their paper applies to UO_3 too, but this is in disagreement with the other data points presented by [Katz and Rabinowitch, 1951] discussed above. I conclude that the [Huttig and von Schroeder, 1922] reference is unreliable for the present work.

D.3   References

J. Danroc, "Evolution Superficielle et Aptitude au Compactage des Poudres de Dioxyde d'Uranium," Doctoral Thesis, l'Institut National Polytechnique de Grenoble, April 1982.

H. R. Hoekstra and S. Siegel, "The Uranium Trioxide-Water System," J. Inorg. Nucl. Chem., Vol. 35, pp. 761-779, Pergamon Press, UK, 1973.

G. F. Huttig and E. von Schroeder, "Uber die Hydrate des Urantetroxyds and Urantrioxyds," 1922.

Joseph J. Katz and Eugene Rabinowitch, "The Chemistry of Uranium: The Element, Its Binary and Related Compounds," National Nuclear Energy Series, Manhattan Project Technical Section, Division VIII - Volume 5, Dover Publications, New York, 1951.

APPENDIX E
DELETED

APPENDIX F

INTERPRETATION OF PNNL DRYOUT EXPERIMENTS

This appendix uses PNNL data for dryout K-basin canister sludge [Abrefah, et al., 1998] to derive best-fit Arrhenius parameters for decomposition. Best-fit Arrhenius parameters are found for each of three decomposition steps as described below.

Abrefah assumed a first-order Arrhenius rate law for each of three decomposition reactions:

$$\frac{dw}{dt} = - K(T) w \qquad \text{(F-1)}$$

$$\ell n\ K = \ell n\ k_o - \frac{Q}{T} \qquad \text{(F-2)}$$

where w = weight of water for decomposition step,
  $K(T)$ = rate constant, min^{-1},
  k_o = pre-exponential factor, inverse minutes,
  Q = activation energy, K, and
  T = temperature, K.

Abrefah's fits (Table F-1) were used to create seven sets of synthetic data. A least squares fit was applied to the synthetic data to determine a best-fit.

Derived values are given in Table F-2. Figures F-1 through F-4 contain plots of Abrefah's individual experiment fits, as well as the derived best-fit.

For example, the rate constant for the first decomposition at CVD, 50°C, is 1.316×10^{-4} min^{-1}, which implies a decomposition half-life of 5,267 minutes or about 88 hours.

Reference:

J. Abrefah, H. C. Buchanan, and S. C. Marschman, "Drying Behavior of K-East Canister Sludge," PNNL-11628, UC-602, Pacific Northwest National Laboratory, Richland, WA, May 1998.

Table F-1: Decomposition Parameters of KE Canister Sludge [Abrefah, et al., 1998]						
TGA Run #	Pre-Exponential Factors, k_0 (min^{-1})			Activation Energies, Q (K)		
	Peak 1	Peak 2	Peak 3	Peak 1	Peak 2	Peak 3
40	2253	56000	15600	5504	7308	7540
41	16000	19900	11500	6010	6750	7350
42	40000	59400	10100	6104	7300	7515
43	24	48100	6700	3687	7550	7700
44	324	28000	4400	5000	7200	7500
45	238	11000	1400	4471	6950	7480
46	326	56700	4513	5003	7630	7754

Table F-2: Best-Fit Arrhenius Parameters for Decomposition		
Step	Pre-Exponential Factor, k_0, (inverse minutes)	Activation Energy, Q, (Kelvins)
1	980	5111
2	34280	7241
3	6162	7548

Figure F-1

CHECK ABREFAH'S PEAK #3 DATA - GET BEST FIT FOR TRANSIENT CALCULATIONS

Pre-exponential, inverse minutes	Activation energy, Kelvins	Evaluate from 150 C to 400 C every 10 C:

$$i = 0..25 \qquad T_i = 273 - 150 - 10 \cdot i$$

15.6   7540

11.5   7350 $j = 0..6 \qquad k_{i,j} = 7 \cdot i - j$

10.1   7515

$K_o = 6.7 \cdot 10^3 \qquad Q = 7700$

4.4   7500

1.4   7480 $TD_{(k_{i,j})} = T_i \qquad K_{(k_{i,j})} = K_{o_j} \cdot e^{-\frac{Q_j}{T_i}}$

4.51   7754

$$VX_{(k_{i,j})} = \frac{1}{T_i} \qquad VY_{(k_{i,j})} = \ln K_{(k_{i,j})}$$

Best-fit values for 150 to 300 C:

$A = \text{intercept}(VX, VY) \qquad K_{ave} = e^A \qquad K_{ave} = 6.162 \cdot 10^3$

$Q_{ave} = -\text{slope}(VX, VY) \qquad Q_{ave} = 7.548 \cdot 10^3 \qquad$ Evaluate best fit: $\quad Y_{ave_i} = \ln\left(K_{ave} \cdot e^{-\frac{Q_{ave}}{T_i}}\right)$
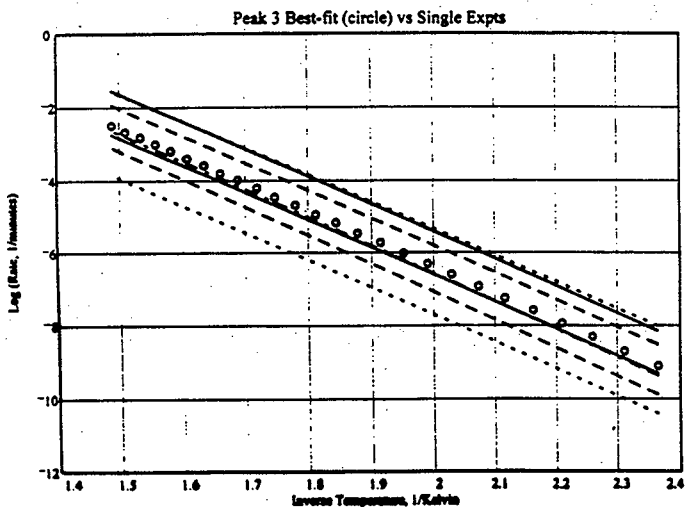

Peak 3 Best-fit (circle) vs Single Expts

Figure F-2

CHECK ABREFAH'S PEAK #2 DATA - GET BEST FIT FOR TRANSIENT CALCULATIONS

Pre-exponential, inverse minutes	Activation energy, Kelvins	Evaluate from 150 C to 300 C every 10 C:

$$i = 0..15 \qquad T_i = 70 - 150 - 10 \cdot i$$

$$j = 0..6 \qquad k_{i,j} = 7 \cdot i - j$$

$$K_o = \begin{bmatrix} 56.0 \\ 19.9 \\ 59.4 \\ 48.1 \\ 28.0 \\ 11.0 \\ 56.7 \end{bmatrix} \cdot 10^3 \qquad Q = \begin{bmatrix} 7308 \\ 6750 \\ 7300 \\ 7550 \\ 7200 \\ 6950 \\ 7630 \end{bmatrix}$$

$$TD_{k_{i,j}} = T_i \qquad K_{k_{i,j}} = K_{o_j} \cdot e^{\frac{Q_j}{T_i}}$$

$$VX_{k_{i,j}} = \frac{1}{T_i} \qquad VY_{k_{i,j}} = \ln K_{k_{i,j}}$$

Best-fit values for 150 to 300 C:

$$A = \text{intercept}(VX, VY) \qquad K_{ave} = e^A \qquad K_{ave} = 3.428 \cdot 10^4$$

$$Q_{ave} = \text{slope}(VX, VY) \qquad Q_{ave} = 7.241 \cdot 10^3 \qquad \text{Evaluate best fit:} \qquad Y_{ave_i} = \ln K_{ave} \cdot e^{\frac{Q_{ave}}{T_i}}$$

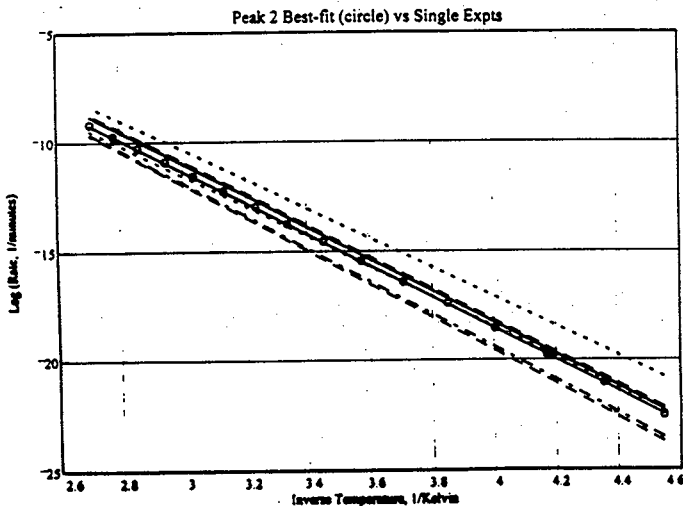Peak 2 Best-fit (circle) vs Single Expts

Figure F-3

CHECK ABREFAH'S PEAK #1 DATA - OMIT TGA # 43, 46 FOR BEST ESTIMATE

Pre-exponential, inverse minutes	Activation energy, Kelvins	Evaluate from 70 C to 220 C every 10 C:

$$i = 0 .. 15 \qquad T_i = 273 - 70 - 10 \cdot i$$

$$j = 0 .. 4 \qquad k_{i,j} = 5 \cdot i - j$$

$$
K_o = \begin{matrix} 2253 \\ 16000 \\ 40000 \\ 324. \\ 238. \end{matrix} \qquad Q = \begin{matrix} 5504 \\ 6010 \\ 6104 \\ 5000 \\ .4471 \end{matrix}
$$

$$TD_{k_{i,j}} = T_i \qquad K_{k_{i,j}} = K_{o_j} \cdot e^{\frac{Q_j}{T_i}}$$

$$VX_{k_{i,j}} = \frac{1}{T_i} \qquad VY_{k_{i,j}} = \ln K_{k_{i,j}}$$

Best-fit values for 70 to 220 C:

$$A = \text{intercept}(VX, VY) \qquad K_{ave} = e^A \qquad K_{ave} = 1.103 \cdot 10^3$$

$$Q_{ave} = \text{slope}(VX, VY) \qquad Q_{ave} = 5.104 \cdot 10^3 \qquad \text{Evaluate best fit:} \qquad Y_{ave_i} = \ln K_{ave} \cdot e^{\frac{Q_{ave}}{T_i}}$$

Half-life at 75 C should be 30 to 60 hours: $\qquad K75 = K_{ave} \cdot e^{\frac{Q_{ave}}{348.15}} \qquad \tau_{75} = 0.693 \cdot K75^{-1} \cdot 60^{-1} \qquad \tau_{75} = 24.328$
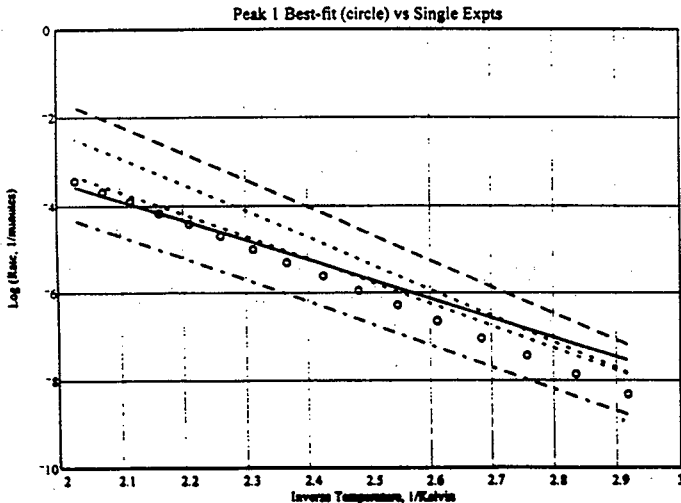

Peak 1 Best-fit (circle) vs Single Expts

Figure F-4

CHECK ABREFAH'S PEAK #1 DATA - GET BEST FIT FOR TRANSIENT CALCULATIONS

Pre-exponential. inverse minutes	Activation energy. Kelvins

Evaluate from 70 C to 220 C every 10 C:

2253	5504
16000	6010
40000	6104
K_o = 24.0 Q = 3687	
324.	5000
238.	4471
326.	5003

$i := 0..15$ $T_i := 273 - 70 - 10 \cdot i$

$j := 0..6$ $k_{i,j} := 7 \cdot i - j$

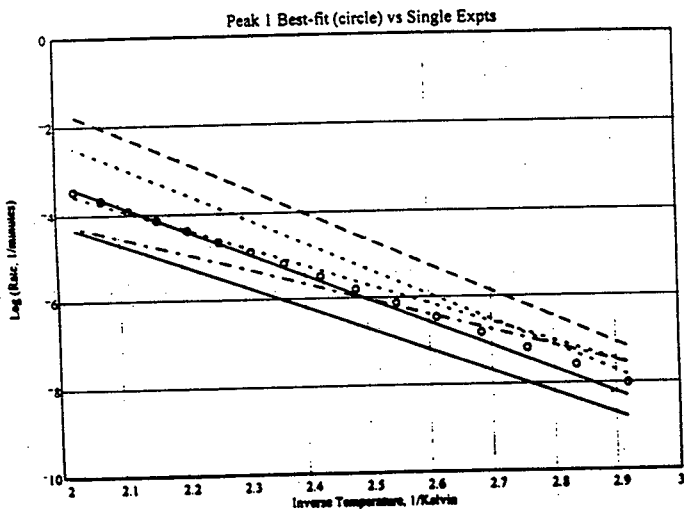$TD_{k_{i,j}} := T_i$ $K_{k_{i,j}} := Ko_j \cdot e^{\frac{Q_j}{T_i}}$

$VX_{k_{i,j}} := \frac{1}{T_i}$ $VY_{k_{i,j}} := \ln K_{k_{i,j}}$

Best-fit values for 70 to 220 C:

$A := \text{intercept}(VX, VY)$ $K_{ave} := e^A$ $K_{ave} = 980.293$

$Q_{ave} := \text{slope}(VX, VY)$ $Q_{ave} = 5.111 \cdot 10^3$ Evaluate best fit: $Y_{ave_i} := \ln K_{ave} \cdot e^{\frac{Q_{ave}}{T_i}}$

Half-life at 75 C should be 30 to 60 hours: $K75 := K_{ave} \cdot e^{\frac{Q_{ave}}{348.15}}$ $\tau_{75} := 0.693 \cdot K75^{-1} \cdot 60^{-1}$ $\tau_{75} = 28.004$

Peak 1 Best-fit (circle) vs Single Expts

APPENDIX G

URANIUM PEROXIDE HYDRATE FORMATION AND DECOMPOSITION

G.1   Purpose and Summary

The purpose of this Appendix is to review literature data on formation and decomposition of uranium peroxide hydrates, $UO_4 \cdot 4H_2O$, and $UO_4 \cdot 2H_2O$.

Two literature sources and recent PNNL data support a conclusion that $UO_4 \cdot 4H_2O$ will easily decompose to $UO_4 \cdot 2H_2O$ during cold vacuum drying conditions which include a proof test at 75°C.

G.2   Formation

$UO_4 \cdot xH_2O$ was prepared by precipitation from uranyl nitrate solution in the three references consulted here: [Huttig and von Schroeder, 1922], [Sato, 1963], and [Boggs and El-Chehabi, 1957]. It is not clear whether significant quantities of UO_4 hydrates can be formed under K-basins conditions.

G.3   Decomposition Literature

The above references agree that $UO_4 \cdot 4H_2O$ easily decomposes to $UO_4 \cdot 2H_2O$ between 25°C and 100°C. Further water loss and eventual decomposition to UO_3 occurs at higher temperatures. There is an obvious water vapor pressure effect for the first stage of decomposition at low temperature, which is exactly as expected from thermodynamic data.

Sato presents a single curve for decomposition of $UO_4 \cdot 4H_2O$ to $UO_4 \cdot 2H_2O$ at room temperature, presumed 25°C, and under vacuum, reproduced as Figure G-1. The half-life for

Figure G-1: Variation of Mol. Ratio H_2O / UO_4 in $UO_4 \cdot 4H_2O$ (specimen 1) With Time of Drying in Vacuum at Room Temperature [Sato, 1963].
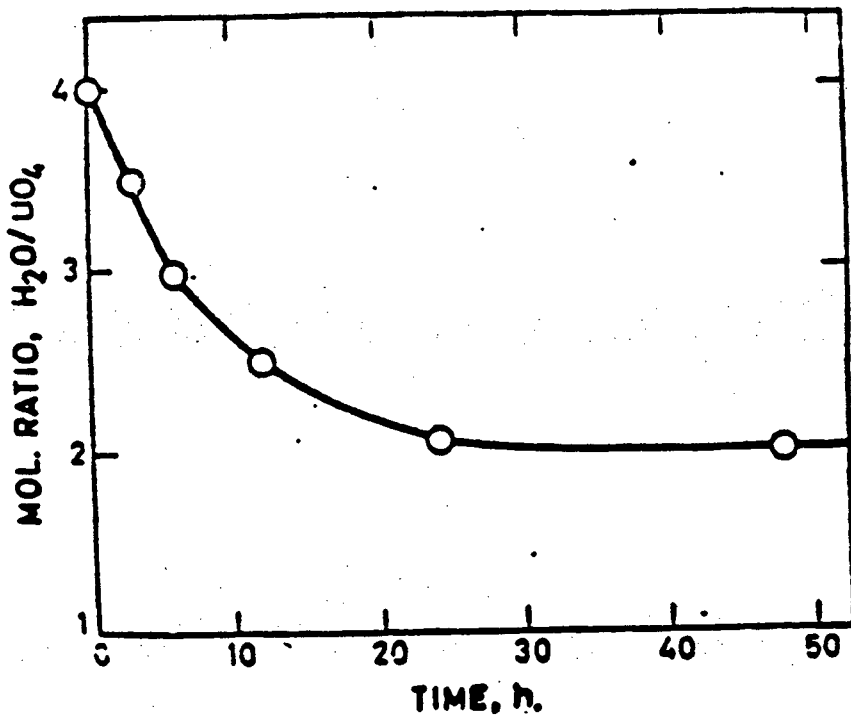
decomposition is about 6 hours and completion occurs at 24 hours. Sato also presents 17 curves for decomposition of UO_4 hydrates with $x = 2$ to $x = 4$ H_2O, where the temperature was raised at 4°C/minute apparently in vacuum. For samples with $x > 2.2$, clear breaks are apparent between the decomposition stages. Very high temperatures, 600°C and above, were required for final dryout and may be attributable to either the relatively quick heatup rate or the presence of surface adsorbed water on precipitated samples of high surface area.

Boggs and El-Chehabi present rate data for $UO_4 \cdot 2H_2O$ decomposition for various temperatures sufficient to formulate a first-order kinetic rate law between 90°C and 150°C. Results in oxygen and air atmospheres were stated to be the same, as were results under 30 torr and 8 torr water vapor partial pressure (about 4 kPa and 1 kPa, respectively). Rate law data of Boggs and El-Chehabi are summarized here:

T, °C	100	120	130	150
k, hr^{-1}	4.4×10^{-4}	4.0×10^{-3}	1.4×10^{-2}	1.3×10^{-1}

Boggs and El-Chehabi are careful to point out "striking disagreement" between their results and those of [Huttig and von Schroeder, 1922]. [Boggs and El-Chehabi, 1957]'s rate constant at 150°C is 0.13 1/hr, so the half-life is 5.3 hours for decomposition, while Huttig and von Schroeder report a rather steep loss of 1.5 moles H_2O at 162 and 163°C. It is worth noting here that Huttig and von Schroeder's work could be interpreted to show this decomposition occurring in about 5 hours. It is perhaps the choice of dwell time at that temperature, which creates the illusion of a congruent decomposition, that led to Boggs and El-Chehabi's objection to the Huttig and von Schroeder data.

Huttig and von Schroeder provide a data table for loss of water from $UO_4 \cdot 4H_2O$ under about 14 - 17 torr water partial pressure, about 2 kPa, and for temperatures up to 450°C. From Figure G-2, loss of the first two moles of H_2O begins at about 50°C. Here one sample was heated and examined after various temperatures were attained, but the heating schedule is not precisely stated, and several data points were taken at 162 and 163°C, but the dwell time was

Figure G-2: Thermal Decomposition of $UO_4 \cdot xH_2O$.
The Solid Line Refers to Moles of Water
The Dotted Line Refers to Moles of Oxygen
[Huttig and von Schroeder, 1922].
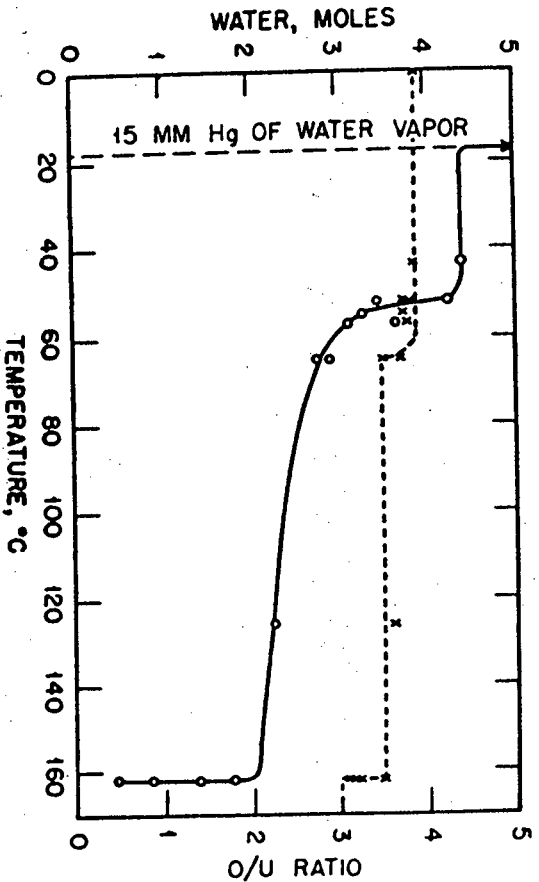
not indicated. It is not clear why several points were taken at about 162°C although this was probably done because the decomposition was observed (or anticipated) to be more rapid. Their data provide an illusion of congruent decomposition at that temperature which was apparently disliked by Boggs and El-Chehabi as discussed above. The actual statement about heating rate was that measurements were taken after intervals of about 10 to 50 minutes, so it is difficult to use these data for kinetic rate laws.

G.4 Recent PNNL Data

Recent data taken by Abrefah at PNNL have been supplied in draft, unqualified form for this Appendix. X-ray diffraction data showed the composition of the grey surface coating on K-basin fuel cladding to be $UO_4 \cdot 4H_2O$, and complete dryout of two samples yielded a mass loss of 23%, consistent with the coating being entirely composed of this hydrate.
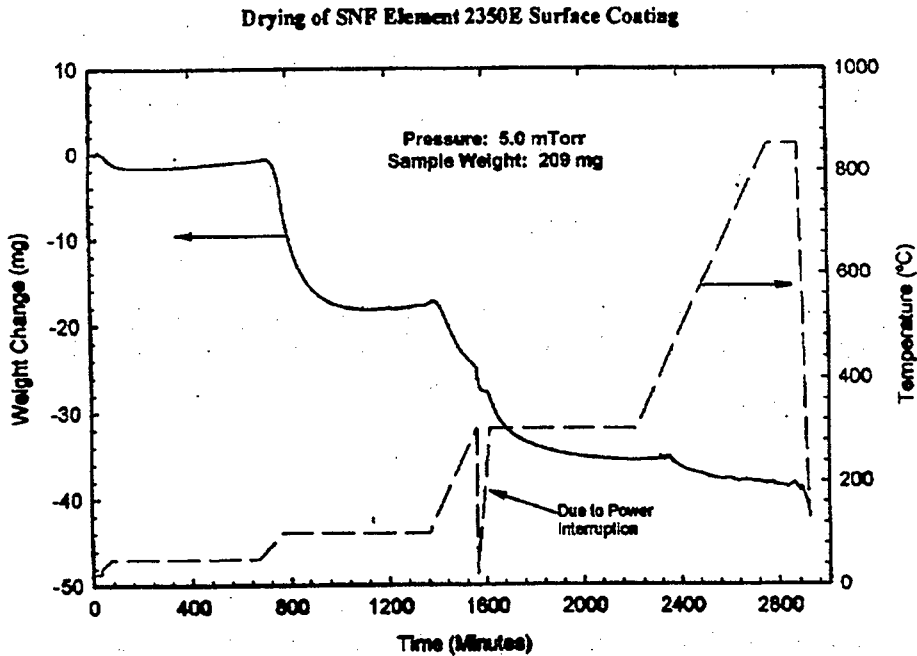
Dryout data taken at a pressure of 5 mtorr and following the time-temperature history used for K-East canister sludge (see Appendix E) are given in Figure G-3. Decomposition of $UO_4 \cdot 2H_2O$ appears to occur as the temperature is raised from 50°C to 75°C, and reaches completion in only several hours at 75°C. Final decomposition occurs when the sample is heated above 75°C.

These data are in very good agreement with literature references for $UO_4 \cdot 4H_2O$ decomposition.

G.5 References

J. E. Boggs and M. El-Chehabi, "The Thermal Decomposition of Uranium Peroxide, $UO_4 \cdot 2H_2O$," J. Am. Chem. Soc., Vol. 79, p. 4258, 1957.

G. F. Huttig and E. von Schroeder, "Uber die Hydrate des Urantetroxyds and Urantrioxyds," 1922.

Figure G-3: Draft, Unqualified PNNL Drying Curve for Surface Coating Believed Composed of $UO_4 \cdot 4H_2O$.

Drying of SNF Element 2350E Surface Coating

Pressure: 5.0 mTorr
Sample Weight: 209 mg

Due to Power Interruption

T. Sato, "Preparation of Uranium Peroxide Hydrates," J. Appl. Chem., Vol. 13, August 1963, pp. 361-365.

APPENDIX H

ADSORBED WATER ON OXIDE SURFACES

H.1   Purpose and Summary

The purpose of this calculation is to quantify a possible range for adsorbed water inventory associated with exposed fuel surfaces. Considering all fuel assembly surfaces and four adsorbed layers, the adsorbed water mass is 0.1 gram. For a sensitivity case of 50 kg of particles with a specific area of $1.2 * 10^6$ cm^2/kg, the adsorbed water mass is still less than 10 grams.

H.2   Calculation

The adsorbed water mass is given by:

$$M = \frac{n\,M\,L\,A}{N_A} \qquad\qquad (H\text{-}1)$$

where: n $=$ Number density of absorption sites, cm^{-2},

N_A $=$ Avogadro's number, 6.023×10^{23} per mole,

M $=$ Molecular weight of water, 18 g/mole,

L $=$ Number of layers, and

A $=$ Surface area, cm^2.

Using a lattice parameter of about 5 angstroms [Katz, Seaborg, and Morss, 1986] and allowing one adsorption site per oxygen atom, i.e., two sites per lattice, yields a site number density of $8 * 10^{14}$ sites/cm^2, or a rounded value of 10^{15} sites/cm^2. Because uranium oxide hydrates could be present on cladding surfaces, the total damaged plus undamaged area of 3,156 cm^2/ assembly is used for $5 * 54 = 270$ assemblies/MCO, yielding $A = 850,000$ cm^2. For a single absorbed layer, the associated water mass is

$$\frac{10^{15} \ \frac{\text{sites}}{\text{cm}^2} \times 18 \text{ g/mole} \times 850,000 \text{ cm}^2}{6.02 \times 10^{23} \ \frac{\text{sites}}{\text{mole}}} = 0.025 \text{ g} \qquad \text{(H-2)}$$

So even if there were 4 layers of adsorbed molecules, the water mass would only be about 0.1 gram.

Particulate can have much higher surface area, as can oxide layers with cracks. The area of particulate can be estimated by:

$$A = \frac{6 \ M_p \ (1 - \phi)}{\rho \ D} \qquad \text{(H-3)}$$

where: M_p = Particulate mass, g,

ρ = Particulate density, g/cm^3,

ϕ = Void fraction, and

D = Particle size, cm.

Taking a particle size of 3 microns, equivalent to the average layer thickness used by [Sloughter, 1998], and a void fraction of 0.4 typical of randomly packed particles, the area per kilogram of particulate is:

$$\frac{A}{M_p} = \frac{6 \ (1 - 0.4) \ (10^3 \text{ g/kg})}{(10 \text{ g/cm}^3) \ (3 \times 10^{-4} \text{ cm})} = 1.2 \times 10^6 \text{ cm}^2/\text{kg} \qquad \text{(H-4)}$$

It is clearly not reasonable to assign such a large specific area to all the particulate in an MCO, since much of this value consists of oxide layers. However, assuming 50 kg of particulate with this surface area yields an adsorption surface area of $6 * 10^7$ cm^2 and an adsorbed water mass for a single layer of 1.8 gram. Hence, multiple adsorbed layers on finely divided particles would still contribute less than 10 grams to an MCO water inventory.

H.3 References

J. J. Katz, G. T. Seaborg, and L. R. Morss, "The Chemistry of the Actinide Elements," Second Edition, Chapman and Hall, New York, 1986.

J.P. Sloughter, "Estimates of Particulate Mass in Multi-Canister Overpacks," HNF-1527, Rev. 2, Numatec Hanford Corporation, Richland, WA, October 1998.

APPENDIX I
K-BASINS SLUDGE PHYSICAL PROPERTY DATA
## DRAFT REFERENCE EXCERPTS

I.1   Purpose and Summary

The purpose of this section is to describe the available sludge property data. Bulk density and particle density are of most interest. Values for K-East sludge physical properties have been compiled and are presented here as graphs that illustrate important trends. Particle densities based on five samples show a range from 3.49 to 7.88 g/cc. The K-East maximum value for bulk density is 2.99 g/cc. Data for K-West sludge area sparse. Only three bulk density values have been reported: 4.18 g/ml, 1.66 g/ml, and 2.49 g/ml. Particles that cling tenaciously have bulk densities exceeding 4 g/cc, implying particle densities of at least 8 g/cc.

I.2   K-Basins Sludge Physical Property Data

K-East basin canister sludge physical property data have been gathered by a number of investigators and compiled by [Makenas, et al., 1997]. Data for the sludge settled bulk density (literal mass divided by volume for a wet sample), water mass and volume fractions (of wet samples), uranium mass and volume fractions (of wet samples), and particle density (the density of dried solids) data are summarized in Figure I-1. The normalized uranium mass fraction used in the figure is the mass fraction within the particles, i.e., the bulk uranium mass fraction divided by one minus the water mass fraction. The following trends are observed:

1.   The water mass fraction and bulk density are correlated, as expected, and
     the lowest observed water mass fraction is 22%.

2.   Particle densities have only been measured for five samples, and range
     from 3.49 g/cc to 7.88 g/cc.

Figure I-1:   K-East Sludge Observed Physical Properties.
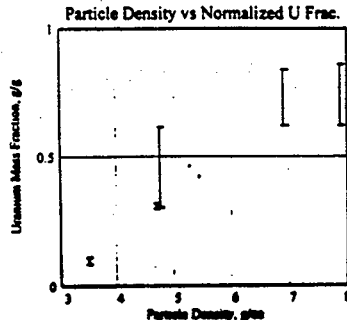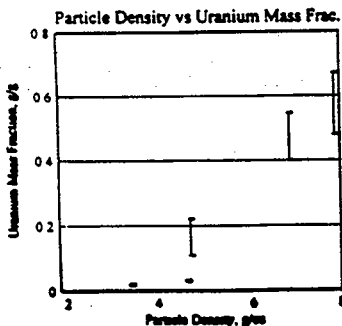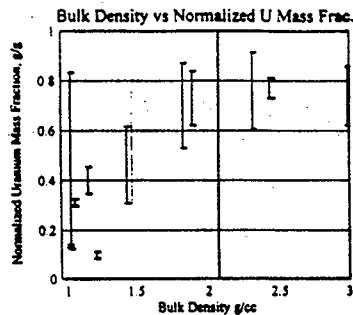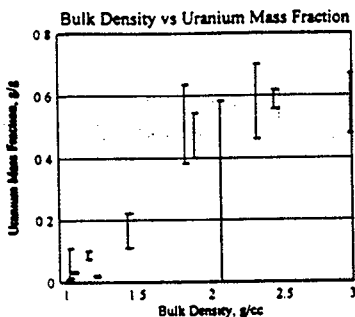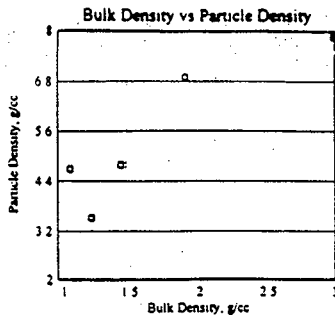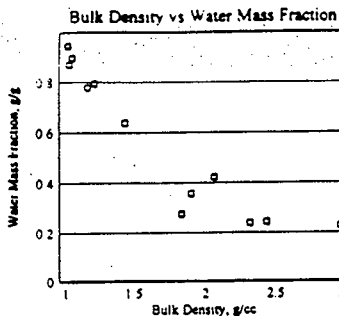
3. Bulk density and particle density are strongly correlated, as physically expected.

4. There is scatter in uranium mass fraction data, and some samples exhibited little uranium.

5. Particle density and bulk density are both correlated with uranium mass fraction and normalized uranium mass fraction. Little uranium is seen in particles with the lowest densities.

6. The normalized uranium mass fraction values are (with the exception of a sample with considerable scatter) below the mass fraction of U in UO_2, 88%. For low bulk densities, these normalized fractions are below the mass fraction of U in $UO_3 \cdot 2H_2O$, 74%.

Data from K-West sludge is sparse at this time. Three settled bulk densities are reported by [Makenas, Baker, and Chastain, 1997]: 4.18 g/ml, 1.66 g/ml, and 2.49 g/ml. One of these values is greater than the K-East maximum value, 2.99 g/ml.

Particulate that clings tenaciously to fuel surfaces appears to have even higher density. Using measured weights and estimated volumes from [Pitner, 1997], Thierry Flament of NUMATEC calculated the bulk densities of samples removed from fuel during subsurface examination as follows:

Element	ID	Description	Volume (ml)	Weight (g)	Density (g/cm³)
6743U	SSL4	Fuel Particulate from Center Breach	1	4.42	4.42
	SSL5	Fuel Particulate from Bottom Breach	< 1	1.68	> 1.68
5427E	SSL1	Fuel Particulate from Top End	3	15.53	5.17
7913U	SSL8	Fuel Particulate from Center Breach	2	8.19	4.09

In all but one case, bulk densities exceeded 4 g/cc, implying the highest particle densities. Figure I-1 suggests, for example, that the particle density would be at least 8 g/cc.

For the case of canister particulate adhering to undamaged or damaged fuel element surfaces, the bounding water content of interest is associated with low density canister material with a high proportion of $A\ell(OH)_3$ and $Fe(OH)_3$. Data from [Makenas, et al., 1997] were reviewed by [Sloughter and Barney, 1998] specifically to identify such compounds. K-East sample data exhibiting the highest possible water content may be summarized as follows:

Parameter	Sample							
	96-08		96-09		96-11U		96-11L	
	µg/g dry	% total as hydrox-ide	µg/g dry	% total as hydrox-ide	µg/g dry	% total as hydrox-ide	µg/g dry	% total as hydrox-ide
$A\ell$	78600	22.72	139000	40.18	139000	40.18	65500	18.93
Fe	72700	13.91	210000	40.18	121000	23.15	256000	48.98
U	385000	49.50	131000	16.84	133000	17.10	77900	10.02
Total (1)	-	88.2	-	100.51	-	86.43	-	80.43
Water % (2)		17%		26%		21.6%		20%
U wt. % (3)		40		8.8		-		9.3
Density, g/ml		1.53		1.2		1.27		1.4
(1) Includes other elements not listed. (2) Derived from % as hydroxide values. (3) Average of four techniques.								

The above selected data represent K-East canister sludge samples with the highest water content and with uranium content below 40%. Available K-West data exhibit uniformly lower water content by about a factor of two (see Figure 3-1). [Sloughter and Barney, 1998] note that typical $A\ell$:Fe ratios in canister sludge are 1:1, while typically the U content is 75%. Also, the average K-East bulk sludge density is about 1.62 g/cm^3 while that of K-West is 2.68 g/cm^3 [Sloughter, 1998]. Clearly, the U content is much lower and particles are of low density when the water content is high.

Other pertinent physical property data are the densities of pure materials:

UO_2	10.95 g/cc
U_4O_9	≈ 11
U_3O_7	11.32
$UO_3 \cdot 2H_2O$	4.83 to 5.0
U	19.05
$UO_4 \cdot 2H_2O$	4.66
$UO_4 \cdot 4H_2O$	5.15

I.3   References

B.J. Makenas, et al., "Analysis of Sludge from Hanford K East Basin Canisters," HNF-SP-1201, UC-2070, September 1997.

B.J. Makenas, R.B. Baker, and S.A. Chastain, "Highlight Report: Gas Generation, Density, and Particle Size of K West Basin Canister Sludge," DESH-9757167, 1997.

A.L. Pitner, "K-Basin Fuel Subsurface Examinations and Surface Coating Sampling," HNF-SD-SNF-TI-060, Rev. 0, DE&S Hanford, Richland, WA, September 1997.

J.P. Sloughter, "Estimates of Particulate Mass in Multi-Canister Overpacks," HNF-1527, Rev. 2, Numatec Hanford Corporation, Richland, WA, October 1998.

Sloughter, J.P., and Barney, G.S., "Identities of Compounds in Spent Nuclear Fuel Coatings and Particulates Sealed in Multi-Canister Overpacks," HNF-2667, Rev. 1 (Draft), Numatec Hanford Corporation, Richland, WA, July 1998.

APPENDIX J
DELETED

APPENDIX K
DELETED

APPENDIX L
CALCULATION NOTE COVER SHEET AND METHODOLOGY CHECKLIST

CALCULATION NOTE COVER SHEET

SECTION TO BE COMPLETED BY AUTHOR(S):

Page ___i_ to _L-3_

Calc Note Number __FAI/98-97_____ Revision Number ___3_____

Title __K-Basins Particulate Water Content, Behavior, and Impact_____

Project __Spent Nuclear Fuel_____

Project Number or
Shop Order ___FND001-14____

Purpose: Post-CVD MCO water content estimates.

Results Summary: High bounding mass 4.8 kg, nominal 1.25 kg.

References of Resulting Reports, Letters, or Memoranda (Optional)

Author(s):
Name (Print or Type)

Martin G. Plys_____

Signature

Completion
Date

__10/21/98__

SECTION TO BE COMPLETED BY VERIFIER(S):

Verifier(s):
Name (Print or Type)

Boro Malinovic_____

Signature

Completion
Date

__10/21/98__

Independent Review or
Method of Verification: Design Review _____, Alternate Calculations __X_, Testing _____
Other (specify) _____

SECTION TO BE COMPLETED BY MANAGER:

Responsible Manager:
Name (Print or Type)

Martin G. Plys_____

Signature

Approval
Date

__10/21/98__

CALC NOTE NUMBER __FAI/98-97_____ REV. __3__ PAGE _i to L-3_

CALCULATION NOTE METHODOLOGY CHECKLIST

CHECKLIST TO BE COMPLETED BY AUTHOR(S) (CIRCLE APPROPRIATE RESPONSE)

1. Is the subject and/or the purpose of the design analysis clearly stated? . . . . . . (YES) . NO

2. Are the required inputs and their sources provided? . . . . (YES) . NO . N/A

3. Are the assumptions clearly identified and justified? . . . . (YES) . NO . N/A

4. Are the methods and units clearly identified? . . . . (YES) . NO . N/A

5. Have the limits of applicability been identified? . . . . (YES) . NO . N/A
   (i.e., Is the analysis for a 3 or 4 loop plant or for a single application.)

6. Are the results of literature searches, if conducted, or other background
   data provided? . . . . (YES) . NO . N/A

7. Are all the pages sequentially numbered and identified by the calculation
   note number? . . . . (YES) . NO

8. Is the project or shop order clearly identified? . . . . (YES) . NO

9. Has the required computer calculation information been provided? . . . . (YES) . NO . N/A

10. Were the computer codes used under configuration control? . . . . YES . NO . (N/A)

11. Was the computer code(s) used applicable for modeling the physical and/or
    computational problems identified? . . . . (YES) . NO . N/A
    (i.e., Is the correct computer code being used for the intended purpose.)

12. Are the results and conclusions clearly stated? . . . . (YES) . NO

13. Are Open Items properly identified? . . . . YES . NO . (N/A)

14. Were approved Design Control practices followed without exception? . . . . . . YES . NO . (N/A)
    (Approved Design Control practices refers to guidance documents within
    NSD that state how the work is to be performed, such as how to perform
    a LOCA analysis.)

15. Have all related contract requirements been met? . . . . (YES) . NO . N/A

NOTE: If NO to any of the above, Page Number containing justification _____

DISTRIBUTION SHEET

To	From	Page 1 of 1
Distribution	Process Engineering	Date 10/22/98

Project Title/Work Order	EDT No. 648613
K-Basins Particulate Water Content, Behavior, and Impact	ECN No. N/A

Name	MSIN	Text With All Attach.	Text Only	Attach./ Appendix Only	EDT/ECN Only
DE&S Hanford					
D. R. Duncan (5)	R3-86	X			
J. R. Frederickson	R3-86	X			
L. H. Goldmann	R3-86	X			
R. P. Omberg	H0-40	X			
K. E. Smith	R3-86	X			
J. A. Swenson	R3-11	X			
SNF Project Files	R3-11	X			
Central Files	A3-88	X			
Numatec Hanford Company					
G. D. Bazinet	S8-06	X			
J. J. Irwin	R3-86	X			
C. R. Miska	R3-86	X			
J. P. Sloughter	H5-49	X			
SESC					
A. L. Pajunen	R3-86	X			